How and why ampliconic genes survive on the human Y chromosome

Authors:
Karol Pal[1], Aleksandra Greshnova[1,2,3], Sukhwan Park[4], Byung June Ko[1], Hana Palova[1], Martin Steinegger[4], Sergei L. Kosakovsky Pond[5], Stefan Canzar[2*], Kateryna D. Makova[1*]

[1] Pennsylvania State University, University Park, PA, USA
[2] University of Regensburg, Regensburg, Germany
[3] Present address: Biozentrum, University of Basel, Basel, Switzerland
[4] Seoul National University, Seoul, South Korea
[5] Temple University, Philadelphia, PA, USA
*Co-corresponding authors

Abstract

The mammalian Y chromosome presents an evolutionary paradox: despite its lack of recombination and propensity for degeneration, it retains multi-copy genes essential for male fertility. To elucidate the reasons and mechanisms for gene survival on the Y in great apes, we integrate telomere-to-telomere assemblies, long-read transcriptomics, protein structure predictions, and selection tests in order to analyze all seven multi-copy gene families on the human Y—*BPY2*, *CDY*, *DAZ*, *HSFY*, *RBMY*, *TSPY*, and *VCY*. First, we show that similar numbers of gene copies are located within palindromes vs. tandem arrays, and that both architectures are equally effective in homogenizing copies via gene conversion. Second, we reconstruct full-length transcripts from PacBio Iso-Seq data from testis across great apes and reveal that transcript diversity arises from both alternative splicing and copy-specific sequence variation. Structural isoform diversity correlates with the number of exons, whereas sequence isoform diversity correlates with the number of gene copies in a family. Third, we find evidence for purifying selection on genes encoding highly ordered proteins (or domains). Thus, highly ordered proteins are conserved across gene copies and species, even in the presence of copy number and RNA isoform variation. Together, our results show that palindrome- and array-mediated homogenization and purifying selection aimed at preserving protein structure jointly enable the survival of fertility-related genes on the non-recombining Y chromosome. These results will inform diagnostic approaches to human Y-linked infertility and studies of the conservation of non-human great apes.

Introduction

Sex chromosomes originated from autosomes independently in different taxa (Zhu, Younas, and Zhou 2025). The proto-Y chromosome in therian mammals acquired the male-determining *SRY* gene approximately 170 million years ago (Veyrunes et al. 2008). This event led to the suppression of recombination with the proto-X chromosome, followed by the accumulation of deleterious mutations and the degradation of the Y chromosome, including the loss of many genes (Skaletsky et al. 2003; Charlesworth 2003). The present-day human Y chromosome consists of two pseudoautosomal regions (PARs), which still recombine with the X chromosome, and X-transposed (acquired through a recent duplication from the X chromosome), X-degenerate (originating from proto-sex chromosomes), and ampliconic (having high sequence identity to itself) regions (Skaletsky et al. 2003). Ampliconic regions harbor multi-copy genes (Y chromosome ampliconic genes, or YAGs) that are expressed in the testis and function in spermatogenesis (Skaletsky et al. 2003), making their preservation critical for reproduction. Highly repetitive ampliconic regions are thought to facilitate the maintenance of functional YAG copies by enabling intrachromosomal recombination (Ohta 1989; Charlesworth 2003; Connallon and Clark 2010; Marais, Campos, and Gordo 2010; Betrán, Demuth, and Williford 2012). Despite this theoretical knowledge, the precise evolutionary dynamics that maintain ampliconic gene integrity across species and how their structural organization affects gene expression and function remain incompletely understood.

Ampliconic regions appear to be a pervasive feature of heterogametic sex chromosomes and are likely critical for maintaining YAGs. These regions are usually organized into two major structural classes—palindromes or tandemly repeated arrays—which arose independently in multiple lineages. Palindromes are inverted repeats where two highly similar sequence arms flank a central spacer. The human Y harbors eight such palindromes (P1-P8) ranging from 30 kb to 2.9 Mb, containing most YAG families (Skaletsky et al. 2003; Trombetta and Cruciani 2017). Palindrome arms maintain >99.9% sequence identity via gene conversion, a type of intrachromosomal recombination (Rozen et al. 2003). Palindromic organization of heterogametic sex chromosomes is frequent across primates (Makova et al. 2024; Hughes, Skaletsky, and Page 2012); the great ape common ancestor already possessed sequences homologous to most human palindromes (Cechova et al. 2020). Palindromes have also evolved in heterogametic sex chromosomes in other species, e. g., in rabbit (Geraldes et al. 2010), some birds, such as sparrows and blackbirds (Davis et al. 2010), and some plants, such as willow (Zhou et al. 2020). In contrast, tandemly repeated arrays (later called “arrays”) are direct repeats of highly similar sequences. They characterize heterogametic sex chromosomes in, for example, mouse (Soh et al. 2014), felids (Brashear, Raudsepp, and Murphy 2018), cattle and sheep (Olagunju et al. 2024), chicken (Huang et al. 2023), and some plants, such as white campion (Hobza et al. 2006). Some species, such as apes, have both palindromes and arrays on their heterogametic sex chromosomes (Makova et al. 2024). However, which organization—in palindromes or arrays—is more efficient at facilitating gene conversion on the Y chromosome remains unexplored. Such information is critical for our understanding of YAG evolution across species and the mechanisms that maintain Y genes in humans.

Palindromes and arrays on the Y are prone to structural rearrangements due to non-allelic homologous recombination (G. P. Smith 1976), resulting in YAG copy number variation. Prior studies documented extensive YAG copy number variation across human Y haplogroups (Ye et al. 2018; Lucotte et al. 2018; Shi, Louzada, et al. 2019; Vegesna et al. 2019) and across species and individuals in great apes (Vegesna et al. 2020). Yet, how copy number variation translates into transcript expression and protein function has remained unclear due to technical challenges in resolving these repetitive regions.

Telomere-to-telomere (T2T) genome assemblies have transformed our ability to fully characterize the structure of Y chromosomes. The T2T assembly of the human Y, generated using long-read sequencing technologies,

resolved its repetitive structure, including YAG family copies (Rhie et al. 2023). The T2T Y chromosome assemblies of six non-human ape species (bonobo, chimpanzee, gorilla, Sumatran orangutan, Bornean orangutan, and siamang) were generated with the same approach, and their YAG families have been completely deciphered (Makova et al. 2024). Population-level studies using T2T methodology analyzed Y chromosomes from 45 men, revealing substantial structural variation (Hallast et al. 2023). There is now a need to characterize the expression of YAG families while accounting for their organization on T2T-resolved Y chromosomes, as many of these genes are essential for reproduction.

Ampliconic genes encode proteins vital for spermatogenesis, making characterization of their expression patterns directly relevant to male fertility (Colaco and Modi 2018; Krausz and Abrardo 2025). Analysis of human YAG families using short-read RNA sequencing established that men with higher gene copy numbers generally exhibit increased expression levels, though substantial inter-individual variation exists (Vegesna et al. 2019). Comparative analysis across great apes revealed that, despite rapid evolution in copy number, expression levels remain conserved, suggesting dosage regulation (Vegesna et al. 2020). However, short-read approaches cannot reliably resolve transcript isoforms originating from gene copies with high sequence identity. Long-read transcriptomics overcomes this barrier by capturing full-length transcript sequences. The IsoCon algorithm was developed specifically to leverage Pacific Biosciences (PacBio) Iso-Seq data to reconstruct transcripts from multi-copy gene families with high copy similarity (Sahlin et al. 2018). Application of this approach to great ape Y chromosomes revealed previously undetectable transcript isoform diversity, including species-specific splicing patterns (Tomaszkiewicz et al. 2023). However, this approach was not informed by the T2T assemblies that fully resolved YAG genomic copies, and thus, it was challenging to assign transcripts to individual gene copies. Therefore, systematic characterization of transcript isoforms across gene copies in ape species and understanding how transcript diversity translates into protein structure remained elusive.

Here, we present a comprehensive analysis of YAGs across great apes, integrating T2T genome assemblies, long-read transcriptomic data, computational protein structure predictions, and selection analyses. In particular, we compared the efficiency of gene conversion in palindromes vs. arrays and determined the extent to which the observed transcript diversity is explained by alternative splicing vs. differences between gene copies. We predicted protein structures for inferred YAG products across species and gene copies, identifying patterns of selection, structural conservation, and divergence with potential functional implications. The results of this study characterize the evolution of YAGs and inform conservation strategies for non-human great apes (all of which are endangered species) and human infertility studies.

Results

Copy number variation and non-Y homologs of Y ampliconic gene families

The availability of T2T genomes for the Y chromosome in human and other great apes (Rhie et al. 2023; Makova et al. 2024) provides an opportunity to evaluate the complete repertoire of YAGs. To identify YAG copies and their non-Y homologs in the reference genomes of bonobo, chimpanzee, human, gorilla, Bornean orangutan, Sumatran orangutan, and siamang (Yoo et al. 2025), we first aligned protein sequences for all protein-coding genes for each species (Thibaud-Nissen et al. 2016) against such sequences from all species using reciprocal BLASTP (Camacho et al. 2009). Two proteins were considered homologs if they had ≥50% amino acid sequence identity over ≥35% of their length (Assis and Bachtrog 2013). We then identified gene families as groups of homologous genes identified through pairwise homology relationships (see Methods for details).

To focus on Y-chromosome multi-copy gene families, we next considered only those with at least two homologs on the Y chromosome in at least one species (Table S1). This resulted in 33 gene families (Table S2). After additional filtering to remove gene families present in only one species, located on PARs, ancient duplications, clustering artifacts, and gene families absent from the human Y chromosome (Tables S1 and S2), we retained seven gene families for subsequent analyses. They represent seven of the nine previously considered human YAG families (Skaletsky et al. 2003): *BPY2, CDY, DAZ, HSFY, RBMY, TSPY,* and *VCY*. The *XKRY* and *PRY* gene families were analyzed in previous studies (Skaletsky et al. 2003; Bhowmick, Satta, and Takahata 2007; Lahn and Page 1997; Cechova et al. 2020; Katrien Stouffs et al. 2004; K. Stouffs et al. 2001; Tomaszkiewicz et al. 2023), but not here because they are annotated as "pseudogene" or "non-coding RNA", respectively, in the latest versions of the T2T-CHM13 genome assembly (Goldfarb et al. 2025) and of all studied ape reference assemblies (Table S3).

We next studied variation in copy number across the seven YAG families, based on our manual curation of YAG annotations (Methods; Table S4) and, when available, across multiple individuals. For humans, copy numbers were inferred (see Methods) from 45 T2T or nearly T2T Y chromosome assemblies (Hallast et al. 2023). For chimpanzee and gorilla, copy numbers were estimated with `AMPLICONE` (Vegesna et al. 2019) from 24 and 18 individuals, respectively, for which short-read data are available (see Methods). For bonobo, Bornean orangutan, Sumatran orangutan, and siamang, we counted the number of copies in their reference assemblies (Makova et al. 2024), as the amount and quality of additional sequencing data for these species were limited. Overall, we found (**Figure 1**) that four gene families (*BPY2*, *DAZ*, *HSFY*, and *VCY*) had consistently low copy numbers (≤10 copies). The remaining three gene families (*CDY*, *RBMY*, and *TSPY*) had a wide range of copy numbers. Variability in copy number for chimpanzees, gorillas, and humans was proportional to the average copy number for the gene family in each species (Figure S1).

To identify significant lineage-specific expansions and contractions of YAG families, we applied `CAFE` (Mendes et al. 2021) while taking median counts for species with multiple individuals analyzed (Tables S5 and S6). Using multiple individuals reduces the influence of outliers that could skew results (e.g., reference HG002 has 45 *TSPY* copies, whereas the median across 45 humans is 32), refining our previously published observations (Makova et al. 2024). We identified significant evolutionary changes in copy number for *CDY, DAZ, RBMY,* and *TSPY* families (Table S7A). *CDY* showed significant expansion in Sumatran orangutan, and *DAZ* in Bornean orangutan. *RBMY* exhibited significant expansion in bonobo. *TSPY* showed contraction in gorilla, expansion in Bornean orangutan, and contraction in Sumatran orangutan. Thus, YAG families experienced substantial copy-number variation both within and across species, with significant family-size contractions and expansions in several lineages.

While determining the complete repertoire of YAGs, we also identified YAG homologs on other chromosomes (**Table 1**). We confirmed the X-chromosome homologs of *RBMY* and *VCY (Bhowmick, Satta, and Takahata 2007; Vallender and Lahn 2004)*. These two gene families displayed the opposite expansion patterns: *RBMX*/*RBMY* expanded mostly on the Y chromosome, whereas *VCX*/*VCY* expanded mostly on the X chromosome (**Table 1**). Additionally, we identified several autosomal *RBMY* homologs: the more closely related genes *RBMXL1-RBMXL3,* which originated by retrotransposition of *RBMX* to autosomes (Lingenfelter et al. 2001; Elliott et al. 2019), and more distantly related genes (*RBMR3*, *CIRBP*, *TRA2A/B*, and *MSI1/2*; Figure S2), which share a highly conserved RNA-binding domain. Consistent with prior literature (Lahn and Page 1999; Saxena et al. 1996), we identified two autosomal paralogs for each of the *CDY* and *DAZ* gene families—*CDYL* and *CDYL2*, and *DAZL* and *BOL*, respectively. No autosomal or X chromosome protein-coding homologs were identified for *BPY2*, *HSFY*, and *TSPY*. *BPY2* (also called *VCY2*) was suggested to be derived from a non-protein-coding gene that gained protein-coding function (Cao et al. 2015). Both *HSFY* and *TSPY*

have homologs on the X chromosome according to prior studies (Bhowmick, Satta, and Takahata 2007; Delbridge et al. 2004); however, we could not detect them because their X-Y divergence occurred prior to or during early mammalian radiation (Bhowmick, Satta, and Takahata 2007; Delbridge et al. 2004; Hughes et al. 2020), resulting in sequence identity below our detection threshold (Note S1). In summary, our analysis of T2T ape genomes confirms the transposition origin of *CDY* and *DAZ,* and the proto-sex-chromosome origin of *RBMY* and *VCY.*

Chromosomal organization and phylogenetic relationships in YAG families

The effects of chromosomal organization on sequence homogenization across YAG copies have not been explored in the T2T genomes. Many human and other ape YAGs are located within palindromes, yet some are organized into tandemly repeated arrays, henceforth called arrays (Makova et al. 2024; Rhie et al. 2023). Each of these two organizations facilitates gene conversion (**Figure 2A**). We hypothesized that being positioned on the opposite arms of the same palindrome provides particularly favorable conditions for homogenization via gene conversion for YAGs (Betrán, Demuth, and Williford 2012; Rozen et al. 2003).

To test this hypothesis, all YAG copies in reference ape genomes were classified as located within palindromes, within arrays, within both palindromes and arrays, or outside of arrays and palindromes (Table S8A). Palindromes were defined with `PALINDROVER` (Makova et al. 2024). Arrays were identified using `AMPLICOVER`, which detects sequence arrays based on genomic spacing between adjacent identical *k*-mers (see Methods). *BPY2*, *CDY*, *DAZ*, *HSFY*, and *VCY* were usually organized into palindromes, *TSPY* into arrays*,* and *RBMY* into both palindromes and arrays (Table S8A). Whereas human possessed one *TSPY* array, bonobo and orangutans had multiple *TSPY* arrays (three in bonobo, two in Sumatran orangutan, and three in Bornean orangutan; Table S8A). In total, across the seven reference ape Y chromosomes, we detected 26 gene-carrying palindromes, each harboring, on average, 6.3 YAG copies, and 14 gene-carrying arrays, each carrying, on average, 10 YAG copies (Table S8C). Altogether, 163 and 140 YAG copies were located within palindromes and arrays, respectively (not counting 11 gene copies present both within an array and a palindrome), and 46 YAG copies were present in neither palindromes nor arrays. Thus, most YAG copies were located within palindromes or arrays. Moreover, both palindromes and arrays held similar amounts of gene copies. However, palindromes were more numerous, and thus each palindrome, on average, carried fewer genes than an array.

To evaluate whether palindromes or arrays lead to greater sequence homogenization, we examined pairwise sequence identity among gene copies within them (**Figure 2B,** Table S9; copies within both arrays and palindromes were excluded from comparisons, and *DAZ* gene copies were excluded due to their unique structure). Pairwise nucleotide identity between genes of the same YAG family and species was calculated based on the number of mismatching bases (excluding gaps) from a pairwise alignment performed with `MAFFT` (Katoh and Standley 2013) in global mode (only gene pairs with a length difference of less than 10% relative to the longer sequence were included in the analysis). The median pairwise nucleotide identity was highest between gene copies on opposite arms of the same palindrome (99.94%), closely followed by that for copies from the same array (99.87%), with no significant difference between these two values (p = 0.2608; two-sided permutation test with 10,000 permutations). There was no difference in median pairwise identity between genes on the same array vs. genes on different arrays (both medians were 99.87%, p = 0.7781). Gene copies located on the same arm of the same palindrome had a significantly lower median identity (99.62%) compared to genes located on the opposite arms of the same palindrome, but this difference was relatively small (difference of 0.32% identity; p = 0.0355; **Figure 2B**). Being located on different palindromes or outside of arrays/palindromes led to a significantly lower pairwise sequence identity (98.73% and 98.99%, respectively) than being located within an array or within the same palindrome (**Figure 2B**). We observed a statistically

significant decrease in identity with increasing distance between copies located in the same array (Figure S3). In conclusion, both palindromic organization and tandem repetition are equally effective at homogenizing YAG sequences.

To further investigate duplication history and gene conversion–driven homogenization within YAG families, we analyzed phylogenetic relationships (using the maximum likelihood approach, see Methods) among paralogs and orthologs within each YAG family (**Figure 2C**). This approach has not yet been applied to T2T genomes, except for the *TSPY* gene family, where phylogeny was still not linked to array versus palindrome organization (Makova et al. 2024). For *BPY2*, nearly identical palindromic gene pairs clustered tightly within species, with chimpanzee retaining only a single copy. *CDY* copies largely formed species-specific clades, though complex repeat structures in orangutans indicated duplications predating speciation with ongoing palindrome-mediated homogenization. Two separate phylogenetic trees were built for the two domains of the *DAZ* gene (**Figure 2C** and Figure S4). *DAZ* showed striking domain-specific patterns: RNA-recognition motifs (RRMs) were highly homogenized and clustered by genus or species (**Figure 2C**), whereas 72- or 90-bp exon repeats (*DAZ* repeats) evolved faster, were less homogenized, and showed weaker phylogenetic structure (Figure S4). *HSFY* copies were homogenized within siamang, human, and gorilla but remained intermingled between orangutan species, reflecting insufficient divergence time for homogenization. *RBMY* exhibited extensive within-species homogenization across palindromes and tandem arrays, with orangutans retaining two distinct gene variants from ancient duplication events. *TSPY*, one of the most abundant Y gene families, was highly homogenized within species despite variable organization across palindromes and arrays. Finally, *VCY* showed evidence of X–Y gene conversion (consistent with (Iwase et al. 2010)), as Y-linked copies did not form a distinct clade from their X-linked homologs. Together, these results highlight palindromes and tandem arrays as powerful drivers of Y-chromosome gene homogenization, modulated by lineage-specific evolutionary histories (see Note S2 for details).

Our phylogenetic analysis revealed that sequence homogenization depends on species divergence time. We detected genus-specific monophyletic YAG clades for most gene families, suggesting homogenization by gene conversion. YAG copies were frequently intermingled between the two species of *Pan* (bonobo and chimpanzee) and between the two species of *Pongo* (Bornean and Sumatran orangutans; **Figure 2C**). In particular, YAG copies were never fully separated into clades for Bornean vs. Sumatran orangutans for any of the studied YAG families. More separation of YAG copies between bonobos and chimpanzees was observed; however, this separation remained incomplete. This observation allows us to estimate the timing of homogenization for YAGs. Given divergence estimates (Makova et al. 2024)—~1 million years ago (MYA) for the two orangutan species, ~2.5 MYA for bonobo and chimpanzee, and ~7 MYA for the *Pan*–human split—our results indicate that the shortest interval is insufficient, the intermediate interval is nearly sufficient, and the longest interval is sufficient to homogenize YAG copies on ape Y chromosomes.

Additionally, based on our results above (**Figure 2B**), we hypothesized that gene copies located on opposite arms of the same palindrome and within arrays would cluster tightly on a phylogenetic tree. Our results indicate that, indeed, the majority of YAG copies located on the opposite arms of the same palindrome form monophyletic clades consisting exclusively of such copies (in 22 out of 26 cases; *DAZ* copies were not considered due to complexity), suggesting high levels of sequence homogenization. Similarly, YAG copies within arrays also form such monophyletic clades for the same genus.

Expression: transcript isoforms

Next, we determined how variability in copy number and DNA sequence differences across gene copies manifests in YAG RNA expression. To answer this question, we reconstructed transcript isoforms from testis

tissue (where these genes are expressed) of the six great ape species analyzed in this study (no testis samples were available for the siamang). We used PacBio Iso-Seq (applied genome-wide and separately targeting these specific gene families) and Illumina short-read RNA-seq to generate long and short transcript reads, respectively (see Methods). We assembled YAG transcriptomes from long and short reads (considered together) with `STRINGTIE` (Shumate et al. 2022). `STRINGTIE` was run in the reference-genome-guided mode, using great ape T2T genomes as references (Makova et al. 2024). We performed variant calling on the PacBio reads to assess sequence variation among transcripts originating from different YAG copies (see Methods for details).

Mechanisms of transcript diversity. We found that transcript diversity results from alternative splicing (i.e., generating *structural isoform variants*) and sequence variation across gene copies (i.e., generating *sequence isoform variants*), and studied how the relative contributions of these two mechanisms differ across gene families and species. The *DAZ* gene family required a separate investigation and is discussed last.

We hypothesized that YAG families with genes containing more exons produce more structural isoform variants. In agreement with this hypothesis, we found a significant positive correlation between the number of non-overlapping exonic regions and structural isoform variant count for YAGs ($r = 0.610$, $p = 9.35\times10^{-4}$, Figure S5A). Altogether, three gene families (*BPY2*, *RBMY*, and *TSPY*) had abundant structural isoform variants (6, 11, and 7, respectively). In contrast, three other gene families (*CDY*, *HSFY*, and *VCY*) each had only two structural isoforms (**Figure 3A**), with *CDY* and *VCY* isoforms segregating by species such that no species contained both variants (**Figure 3B**), whereas most species contained both *HSFY* isoforms.

We next hypothesized that gene families with higher copy number have more sequence isoform variants. In agreement with this hypothesis, we found a significant positive correlation between copy number count and the number of sequence isoform variants ($r = 0.688$, $p = 1.02\times10^{-4}$, Figure S5B). High sequence isoform variant diversity was observed for all high-copy-number gene families: *TSPY*, *RBMY*, and *CDY* in most species. In contrast, *BPY2* and *VCY* showed little to no sequence isoform variation within species (across all species, **Figure 3B**), consistent with these gene families having low copy number (**Figure 1**). A similar pattern was observed for bonobo *CDY*, human *HSFY*, and gorilla *TSPY* (**Figure 3B**)—all of which also have low copy numbers (**Figure 1**).

Transcript isoforms for each gene family. We next combined information about structural and sequence isoform variants to detect distinct transcript isoforms and studied their distribution across species for each gene family (Additional Data File 1; **Figure 3B**). Among genes consistently expressed across species, *TSPY* and *RBMY* showed the greatest diversity in both structural and sequence isoforms. *TSPY* structural isoform variation was driven mainly by intron retention, with all species strongly favoring the same structural isoform (Isoform 32; **Figure 3B**). *RBMY* transcript diversity was concentrated in a 111-bp repeat region and, to a lesser extent, alternative splicing of the 5′ untranslated region (UTR), with clear species-specific isoform preferences (Isoform 35 in gorilla, Isoform 10 in human, and Isoform 14 in bonobo and chimpanzee; **Figure 3B**). Notably, orangutans expressed unique *RBMY* isoforms in which a ~550-bp deletion removes one 111-bp repeat exon but includes a different 111-bp repeat skipped in other species due to a degenerate splice site (Figure S6).

Similar trends were observed between *CDY* and *HSFY*, where transcript diversity was dominated by sequence rather than structural variation. *CDY* showed copy number expansion in orangutans and, to a lesser extent, chimpanzee, accompanied by high sequence isoform diversity. Orangutans also exhibited a divergent *CDY* structural isoform containing an earlier initiation codon (Figure S7). *HSFY* was expressed as two structural isoforms supported by multiple sequence variants in all species except gorilla (**Figure 3B**).

BPY2 and *VCY* were each expressed in only a few species. *BPY2* showed multiple sequence variants but only one structural isoform in human and a single isoform in gorilla. *VCY* exhibited one human-specific and one *Pan*-specific structural isoform, with sequence variation detected only in humans.

DAZ isoforms. *DAZ* isoforms in all species (**Figure 3C)** carried up to three RRMs and a tail of tandemly repeated *DAZ* repeats of variable count (from two in Bornean orangutan to 19 in human), which we studied with a separate approach (see Methods for details; Additional Data File 2). The only exception to this pattern was observed in the *Pongo* lineage, where *DAZ* repeats were sometimes also interspersed between RRMs. In human, we detected isoforms comprising all the *DAZ* repeat sequences previously described in (Fu et al. 2015), demonstrating the precision of our *DAZ* repeat recovery method (Additional Data File 2). In summary, using long-read sequencing, we reconstructed full-length transcripts of great ape YAG families—one of the most complicated repetitive regions of the genome.

Transcript expression levels. To evaluate the effect of our reference-augmented transcriptome on capturing YAG expression in great apes, we mapped testis short-read RNA-seq data to it and (separately) to the standard NCBI RefSeq coding sequence (CDS) set. Expression estimates were compared at the YAG family level (separately for each species) to assess whether the reference-augmented transcriptome recovered additional signal (Table S10). Most genes were unaffected by the inclusion of novel transcripts. However, in some cases, the number of mapped reads increased, most notably for *DAZ* in human and Bornean orangutan. In other cases, TPM (Transcripts Per Million) values changed despite identical read counts, as observed for *TSPY* in Bornean orangutan (Figure S8; Table S10). Although the changes were not substantial, we demonstrate that the choice of transcript library can affect RNA-seq expression level analysis results.

Using the reference-augmented transcriptome, we found substantial species-specific heterogeneity in YAG family expression patterns (Figure S8). *VCY* was the most highly expressed family in chimpanzee and bonobo, *HSFY* dominated in human and Sumatran orangutan, and *TSPY* showed the highest expression in gorilla and Bornean orangutan. Overall, these results suggest that expression estimates are sensitive to transcriptome choice and that accurately modeling YAG transcript structures is important for interpreting RNA-seq data.

Protein structure predictions

We next asked how RNA transcript diversity is translated into protein isoform diversity. Overall, based on sequence, and as expected due to the presence of synonymous variants, there were fewer predicted protein isoforms (later called ‘protein isoforms’) than observed transcript isoforms (**Figure 4B**). Using `COLABFOLD` (Mirdita et al. 2022), we predicted protein structures of all unique protein isoforms. Color-coded local confidence scores (pLDDT) of the predicted protein structures were plotted in **Figure 4A**. Among seven YAG families analyzed, five (*CDY*, *DAZ*, *HSFY*, *RBMY*, and *TSPY*) had high confidence scores at least over portions of their protein sequences, whereas two (*BPY2* and *VCY*, Figure S9A-B) had low confidence scores, suggesting intrinsic disorder (*VCY*) or low confidence in the predicted structure (*BPY2*).

The predicted protein isoform structures were clustered using `FOLDSEEK` (van Kempen et al. 2024), assigning similar structures to a single representative protein structure via structural alignment (Table S11; **Figure 4B**). Despite their high transcript diversity (**Figure 3B**), the highly copious *CDY*, *RBMY*, and *TSPY* families each maintained similar protein folding structure across great apes (**Figure 4B**). For *CDY*, most isoforms were >600 amino acids long and contained two highly ordered domains (**Figure 4C**): the chromodomain near the N-terminus and a catalytic domain near the C-terminal tail (Dorus et al. 2003). Both domains showed high pLDDT scores (>90), suggesting highly ordered structures. Among 24 *CDY* protein isoforms predicted in our data, 21 clustered together, and the three remaining proteins (one in gorilla and two in human) each had

distinct predicted structures. The *RBMY* protein contains one highly ordered domain—an N-terminal RNA-Recognition motif (**Figure 4C**)—found in a number of RNA-binding proteins that mediate RNA interactions (Elliott 2004). Of the 42 predicted *RBMY* protein structures, 35 formed a single cluster encompassing structures predicted in all great apes (**Figure 4B**), suggesting conserved folding. The *Pongo*-specific *RBMY* copies (Figure S9C) formed a secondary cluster together with protein isoforms from gorilla and bonobo. The *TSPY* gene family produced 34 distinct protein isoforms grouped in four clusters (**Figure 4B**). The largest cluster C2 (29 isoforms) mostly grouped protein isoforms originating from transcript Isoform 32 and had a highly ordered predicted structure comprising exons 1 through 5. One smaller cluster (C3), produced by three protein isoforms, consisted of protein derivatives of Isoform 37, which contains a read-through intron between exons 4 and 5; note that this region is not predicted to form an ordered structure (**Figure 4A)**.

For *DAZ* structure predictions, the RRMs had consistently high pLDDT scores, while the scores of *DAZ* repeats were usually lower (Figure S10). Protein isoforms clustered by the number of RRMs present (one, two, or three), forming three distinct large clusters comprising six, eight, and nine isoforms, respectively (**Figure 4B**). The two transcript isoforms of the *HSFY* gene shared one large, highly ordered domain (**Figure 4C**). Additionally, *HSFY* protein isoforms formed one gorilla-specific cluster (with four isoforms), two clusters including human and Sumatran orangutan isoforms (with two isoforms per species), and one singleton including a Bornean orangutan isoform.

In conclusion, we observed that the most copious families (*CDY*, *RBMY*, and *TSPY*) maintained a conserved protein structure, with the majority of protein isoforms forming a single dominant cluster. This is despite substantial transcript diversity at the sequence (*CDY*), structural (*TSPY*), or both (*RBMY*) levels. In cases of *TSPY*, *DAZ*, and *HSFY*, protein clusters usually corresponded to the same transcript structural isoforms. However, *CDY* and *HSFY* generated some protein isoforms derived from identical transcript structural isoforms that nonetheless grouped into distinct protein structure clusters, underscoring that both structural and sequence-level transcript variation contribute to the diversification of protein architecture.

Selection on protein-coding sequences

To analyze selection acting on YAG families, we examined the nonsynonymous-to-synonymous rate ratio (*dN/dS)* in YAG families with `HYPHY` (Kosakovsky Pond et al. 2020) (see Methods for details). Here, we improved our previous analysis (Makova et al. 2024) by including all individual YAG copies (rather than analyzing consensus protein-coding sequences per species) and the closest non-Y homologs, and by applying both branch- and site-specific models.

We found that, in general, all ampliconic genes evolve under either neutrality or purifying selection (**Table 2**). The evolution of three gene families—*BPY2*, *TSPY*, and *VCY*—was consistent with neutrality (*dN/dS* was not significantly different from 1). Purifying selection was statistically significant for *CDY*, *HSFY*, and *RBMY*. For *DAZ*, the selection mode depended on the gene region analyzed, consistent with prior literature (Bielawski and Yang 2001). Namely, we detected evidence of purifying selection within the RRM region, whereas the evolution of *DAZ* repeats was consistent with neutrality (**Table 2**).

We observed significant variability in selection pressure (i.e., significant branch-heterogeneity test results) across branches for *CDY* and *RBMY*. However, no individual branch displayed statistically significant evidence of positive selection for *CDY*, and only one such branch was detected (with aBSREL analysis (M. D. Smith et al. 2015) in *RBMY* (it led to one gene copy in gorilla; Figure S11). Using the MEME model (Murrell et al. 2012), we identified 27 sites evolving under episodic positive selection. Such sites were present in all genes but *BPY2*

and *HSFY*. *RBMY* had the most such sites (15), followed by *CDY* (six). We further evaluated these sites in the context of protein structure.

Out of 27 MEME-predicted sites with episodic diversifying selection found across five genes (**Table 2**), seven were predicted to affect protein function with high confidence (Table S12), according to `SIFT` (Sim et al. 2012) (**Figure 4C**): three in *CDY*, two in *RBMY*, and one in *TSPY***.** Within each YAG family and species, in most cases, mutant protein isoforms with predicted functional changes are likely present with other protein isoforms derived from their wild-type counterparts (Figures S12-S17). Thus, the original function will still be preserved by the latter protein isoforms. An exception is an isoform with a mutation leading to an amino acid substitution (Met -> Thr) at residue 475 for the *CDY* protein in chimpanzee (Figure S18), where the mutant variant with the predicted functional consequence is the only form for all gene copies in this species; this case warrants further investigation with functional experiments.

Discussion

This study presents the first comprehensive integration of T2T genome assemblies, long-read transcriptomics, computational protein structure prediction, and selection tests to characterize YAGs across great apes. By leveraging these data and analyses, we uncovered the evolutionary history of these multi-copy gene families and evaluated the mechanistic basis and reasons for their survival on the largely non-recombining Y chromosome.

Palindromes and tandemly repeated arrays represent equivalent evolutionary solutions for YAG homogenization. An important question in Y chromosome biology is whether palindromic or array organization more effectively facilitates gene conversion—the intrachromosomal recombination process that maintains high sequence identity among gene copies while rescuing the functional ones. To address this question thoroughly, one needs to use fully resolved and complete assemblies, as previous Y chromosome assemblies have frequently had palindromes, and likely also arrays, collapsed (Cechova et al. 2020). Here, for this purpose, we utilized ape T2T Y-chromosome assemblies, which have only recently become available (Rhie et al. 2023; Makova et al. 2024). Our analysis revealed that tandem arrays and palindromes achieve comparable levels of sequence homogenization among YAG copies. Moreover, we found that approximately the same number of YAG copies is organized into each of these two structural repeat classes in the apes studied. Our results agree with previous studies demonstrating that YAG copies positioned on opposite arms of the same palindrome are nearly identical (Hallast et al. 2013), whereas those located at nonsymmetrical positions within a single palindrome, or on different palindromes, show lower sequence identity (Bhowmick, Satta, and Takahata 2007). Our findings support the notion that gene conversion between tandem direct repeats can proceed through homologous recombination (Grondin, Papadopoulou, and Ouellette 1993; Manz et al. 1993; Xue and Tyler-Smith 2011). Such homogenization on the Y chromosome may occur between sister chromatids. Thus, our results suggest that palindromes and arrays represent alternative but functionally equivalent solutions to the challenge of maintaining genes without interchromosomal recombination.

Transcriptome diversity reflects gene structure and copy number. Our analysis revealed extensive isoform diversity within each YAG family, with the number of distinct transcripts exceeding gene copy number. We demonstrated that this diversity arises from two distinct mechanisms, with their relative contributions varying across gene families. Structural isoform diversity, generated through alternative splicing, correlated with the number of exons per gene. As a result, gene families with many exons (*BPY2*, *RBMY*, and *TSPY*) exhibited abundant structural variants, whereas genes having fewer exons (*CDY*, *HSFY*, and *VCY*) each produced only two structural isoforms. Sequence isoform diversity, reflecting copy-specific variants, correlated

with gene copy number. Consequently, high-copy families (*TSPY*, *RBMY*, and *CDY*) showed extensive sequence variation, while low-copy families (*BPY2* and *VCY*) exhibited minimal sequence diversity across their transcript isoforms. A positive correlation between the number of isoforms and the number of exons was shown in an earlier study (Leung et al. 2021). A correlation between the number of gene copies and the number of sequence isoform variants—which would have been difficult to evaluate accurately before the availability of T2T genomes—to the best of our knowledge, represents a novel finding. For the *DAZ* gene family, transcripts varied in both the number of RRMs and the composition of highly similar *DAZ* repeats. This structural complexity might underlie the functional versatility of *DAZ* in spermatogenesis. In general, the results of our study do not fit one of the three previously described evolutionary models of the interplay between gene duplication and alternative splicing in generating transcript isoform diversity (Iñiguez and Hernández 2017). We propose a new model in which transcript diversity—both at the sequence and structural levels—is relatively conserved among gene copies due to frequent gene conversion on the Y chromosome.

Our use of T2T assemblies for long-read transcript mapping produced fewer, but longer, transcripts than the reference-free IsoCon approach (Table S13) we previously applied (Tomaszkiewicz et al. 2023). This difference can be attributed to the fact that mapping transcripts to the T2T genome results in more accurate full-length transcript reconstruction. We have shown that the availability of such an improved transcriptome affects the estimation of YAG expression levels, revealing some species-specific expression patterns.

From transcripts to protein clusters. Despite extensive transcript diversity, we predicted only a limited number of protein structure clusters with `COLABFOLD` (Mirdita et al. 2022). Indeed, there were fewer predicted protein isoforms than transcript isoforms due to the presence of synonymous variants, and, for all YAG families, protein isoforms formed one or just a handful of clusters with similar structure. This suggests substantial structural conservation among protein isoforms originating from each YAG family.

Previous studies have shown that men with high YAG copy numbers generally exhibit increased YAG transcript levels (Vegesna et al. 2019). However, we previously demonstrated that overall YAG transcript expression levels are conserved across great apes despite rapid copy-number evolution (Vegesna et al. 2020). In contrast, our current study shows some variation in YAG expression levels across the same great ape species (Figure S8). Our protein structure predictions and clustering provide a more complex picture: structurally conserved proteins are expected to perform equivalent functions, so increasing copy number directly increases functional transcript output and likely protein output while maintaining the same molecular activity.

Selection maintains function through structure conservation in several ampliconic gene families. Our selection analysis revealed a clear dichotomy among YAG families, providing insight into why the Y chromosome has retained these genes despite its overall degeneration. Three gene families—*CDY*, *HSFY*, and *RBMY* showed evidence of purifying selection. In contrast, the evolution of three other families—*BPY2*, *TSPY*, and *VCY*—was consistent with neutrality. Remarkably, this pattern correlates with protein structure: families evolving under purifying selection encode proteins with highly ordered domains and high AlphaFold confidence scores, whereas *BPY2* might encode ordered proteins but with low confidence scores, and *VCY* encodes intrinsically disordered proteins. *TSPY* represents an intermediate case where protein structure is ordered and conserved despite neutral sequence evolution.

The *DAZ* gene family illustrates how selection pressure can vary across different functional domains within a single gene. The RRM domains, which mediate RNA binding, showed significant purifying selection and were predicted to be highly ordered, whereas the less ordered *DAZ* repeat region evolved neutrally. This domain-specific pattern, consistent with prior work (Bielawski and Yang 2001), suggests that protein-RNA

interactions are functionally constrained, whereas *DAZ* repeats are less constrained (or we lack the power to detect selection acting on them due to their short length).

Therefore, highly ordered proteins and domains require a specific structure for their function and, in general, evolve under purifying selection, which maintains their structure and function. Disordered proteins and protein domains usually do not experience such sequence constraints and, as a rule, evolve neutrally. The intrinsically disordered proteins encoded by *BPY2* and *VCY* may represent a distinct functional class in which disorder itself is functionally relevant, though their roles in spermatogenesis remain poorly characterized (Tse et al. 2003; Wong et al. 2002; Choi et al. 2007; Shi, Massaia, et al. 2019; Zou et al. 2003; Taguchi et al. 2014). It is also possible that *BPY2* and *VCY* are less functionally constrained because they are on the path to becoming pseudogenes.

Evolution of YAGs. Our results are consistent with other studies investigating the evolution of YAG families. For instance, YAG families in felids were found to be conserved despite extensive structural variation (Brashear, Raudsepp, and Murphy 2018). Simulations suggested that gene conversion plays an important role in the conservation of essential duplicated genes (Connallon and Clark 2010), and our data support this claim. Moreover, the theory was recently extended to duplicated genes on the Y in the context of Muller's ratchet (Sakamoto and Innan 2022). In this framework, our results, based on protein structure prediction and clustering, as well as our selection analyses demonstrating purifying selection in several YAG families, strongly argue that gene conversion prevents duplicated genes from losing their function. This scenario is consistent with simulation results under additive dosage effects on fitness (Sakamoto and Innan 2022)—a prediction that should be evaluated in future studies evaluating fitness effects of YAGs with different copy numbers.

Additionally, theoretical models predicted that palindromic organization may accelerate adaptive evolution by increasing targets for beneficial mutations while enabling purging of deleterious variants through gene conversion (Betrán, Demuth, and Williford 2012). In agreement with this prediction, we detected episodic positive selection at multiple sites of YAGs, particularly in *RBMY* and *CDY*, indicating that these gene families experience both purifying and diversifying selection at different positions. Moreover, our `SIFT` (Sim et al. 2012) analysis suggested that sequence variability at several sites evolving under positive selection may affect protein function.

One can draw a parallel between the evolutionary dynamics of ampliconic genes and meiotic drive systems—selfish genetic elements that bias their own transmission (Martí and Larracuente 2023). Sex chromosomes lacking recombination are particularly prone to intragenomic conflict, where segregation distorters trigger arms races between driving and suppressing alleles (Swanepoel and Mueller 2024). The multi-copy organization of YAGs may have originated through such conflicts, with gene amplification providing dosage-sensitive responses to drive elements. Indeed, such intragenomic conflicts were suggested to result in genetic redundancy (Martí and Larracuente 2023). Multi-copy gene family evolution on primate Y chromosomes shows recurrent amplification and loss at rates higher than those on autosomes, consistent with intragenomic conflict operating at sex chromosomes (Ghenu et al. 2016). Recent work on mouse *t*-haplotypes demonstrates that ampliconic sequences are a defining feature of selfish chromosomes, with amplicon acquisition marking the origins of transmission distortion (Swanepoel et al. 2025).

Integration: from genome to function. Overall, our results, as well as those from other studies (e.g., (Lucotte et al. 2023; Vegesna et al. 2019, 2020; Ye et al. 2018)), indicate high copy-number variation for YAGs in humans and apes, and here we show variation in their transcript expression at the level of isoform composition and transcript levels. Yet, here we demonstrate that their protein structures remain conserved. Our findings may resolve this paradox and suggest a buffering system: gene conversion maintains sequence identity among

functional copies within palindromes and arrays; alternative splicing and gene duplication generate isoform diversity from multiple gene copies; and selection maintains conservation of protein structure and, consequently, function, despite some sequence divergence. This multi-level buffering enables the Y chromosome to tolerate substantial DNA sequence and structural variation on this non-recombining, highly mutable chromosome (Makova and Li 2002; Bergeron et al. 2023), while preserving spermatogenic functions essential for male fertility. Measuring protein levels will add the last missing piece to this puzzle.

Implications for human infertility and great ape conservation. Deletions of ampliconic genes, particularly within the AZF (Azoospermia Factor) regions containing *DAZ*, are established causes of spermatogenic failure associated with human male infertility (Krausz and Abrardo 2025). However, standard genetic testing assesses only the presence or absence of gene families, not copy number, isoform composition, or expression levels (Colaco and Modi 2018). Our finding of transcript diversity among great apes suggests variation in transcriptome expression profiles across men, which may influence spermatogenic efficiency independently of gross deletions. Future clinical studies should consider which isoforms are expressed and at what levels. More precise molecular characterization may enable better prediction of fertility outcomes and inform therapeutic strategies.

All non-human great apes are endangered and rely on captive breeding programs, whose success depends on male fertility. However, the genetic factors contributing to great ape spermatogenesis are not well understood. Our analysis of YAG copy number variation, transcript diversity, and species-specific expression patterns provides a foundation for assessing their reproductive health. Significant inter-individual variation in copy number, observed here in chimpanzees and gorillas, suggests that some males might carry YAG configurations linked to reduced fertility. Establishing the normal range of YAG variation in other species (bonobo and orangutans) will be important in future studies. Furthermore, conservation of YAG protein structures despite sequence divergence indicates that human-based functional assays may be applicable to other great apes, supporting comparative reproductive studies.

Methodological advances. This study demonstrates the power of combining T2T assemblies with long-read transcriptomics, protein structure prediction, and selection testing for characterizing repetitive gene families. While working towards this goal, we developed the following new methods. First, we developed a new *k*-mer-based method to detect tandemly repeated arrays. Second, we developed a novel method to resolve transcriptome diversity of multi-copy genes at both the structural and sequence isoform levels, while incorporating T2T assemblies in the analysis. Third, our approach enabled the characterization of transcripts from the *DAZ* gene family at unprecedented detail, distinguishing highly similar copies with complex internal repeat structures. Previous studies could not fully characterize the repeat composition of individual *DAZ* isoforms. Our approach successfully overcame this limitation and detected novel isoforms, including *DAZ* transcripts with three RRMs in most species, including humans—expanding the known diversity of this clinically important gene family (such isoforms were not detected previously according to https://www.ncbi.nlm.nih.gov/gene/1617, accessed April 8, 2026).

Limitations. Several limitations should be acknowledged. First, our transcriptomic data are derived from one individual per species, limiting a comprehensive assessment of intraspecific variation in expression patterns. Second, our transcriptome data originate from different individuals than those used for the T2T reference genome reconstruction, preventing a direct one-to-one transcript-to-copy mapping. While acknowledging this limitation, we would like to highlight that collecting matching data would be very challenging. T2T genome sequencing requires a cell line that can be grown to tens of millions of cells, whereas transcriptome characterization would require fresh tissues. In the future, testis cell type-specific lines would have to be established for great apes, which are all endangered (this will be a major undertaking). Third, while

COLABFOLD (Mirdita et al. 2022) predictions achieve near-experimental accuracy for many protein families (Jumper et al. 2021), predictions may be less reliable for intrinsically disordered proteins and regions. The low confidence scores for *BPY2* and *VCY* likely reflect genuine disorganization rather than prediction failure, but functional implications remain uncertain. Fourth, our analysis focuses on transcript structure and predicted protein properties but does not directly assess protein abundance or functional activity, which may differ from transcript levels due to post-transcriptional regulation. This line of research should be addressed in future work.

Methods

Versions of genome assemblies and NCBI annotations. We used the following versions of genome assemblies: GCF_009914755.1-RS_2024_08 (human CHM13+Y), GCF_029281585.2-RS_2024_02 (gorilla), GCF_029289425.2-RS_2024_02 (bonobo), GCF_028858775.2-RS_2024_02 (chimpanzee), GCF_028885655.2-RS_2024_02 (Sumatran orangutan), GCF_028885625.2-RS_2024_02 (Bornean orangutan), and GCF_028878055.3-RS_2024_07 (siamang).

Assigning genes to gene families. YAG gene families and their homologs were determined for genes from gene annotations provided by NCBI for the genome assemblies listed above. In more detail, a BLASTP (Camacho et al. 2009) database was created from protein sequences of all protein-coding genes of all species. For each gene, the longest protein isoform was selected. For each species, all protein-coding genes were queried against this database using BLASTP (Camacho et al. 2009). Two genes were considered homologs if they reciprocally had at least 50% amino acid sequence identity over at least 35% of their protein lengths (Assis and Bachtrog 2013). Homologous genes were transitively clustered into gene families by identifying connected graph components. If genes (nodes) A and B were identified as homologs (connected by an edge), and so were genes B and C, then genes A, B, and C were assigned to the same gene family. We initially identified 33 gene families with ≥2 Y-linked copies in at least one species. We further filtered these gene families (Table S2) to retain only those with Y-linked copies in at least two species. Additionally, we excluded families located on PARs, *RPS4Y* paralogs due to their ancient divergence (Andrés et al. 2008), five instances of clustering artifacts (genes A and C linked through an intermediary gene B which shared domains with both A and C, while A and C did not share domains; Additional Data File 3), and families absent from the human Y chromosome. This resulted in seven gene families for further analysis (Table S2).

Manual curation of individual YAG copies. Highly similar multi-copy genes and pseudogenes can be incorrectly annotated and misidentified. In (Makova et al. 2024), we addressed this issue by combining multiple annotation sources and manually curating YAGs in great apes. Since this publication, we have continued working with the NCBI gene annotation team to further curate YAGs of all seven ape species we studied in (Makova et al. 2024) and here. Genes and pseudogenes from the same YAG family and the same species, located within the same palindrome or the same array, were aligned with MAFFT v7.526 (Katoh and Standley 2013). When a reading frame in a pseudogene (based on the splice pattern of a homologous protein-coding gene copy) resulted in a transcript without premature stop codons or frameshifts, a change from a pseudogene to a protein-coding gene was proposed. Similarly, truncated copies of annotated protein-coding genes were flagged, and a change from a protein-coding gene to a pseudogene was proposed. These suggestions were reviewed by NCBI (Additional Data File 4) and incorporated into the most recent NCBI Reference Sequence Database (RefSeq). The GFF files resulting from such a manual curation of YAGs are available as Additional Data File 5, accession numbers of all protein-coding genes considered are in Table S14.

Copy number estimation from additional human Y chromosome assemblies. The CDS sequences of all YAG copies annotated on the human reference Y chromosome (HG002) were mapped to the 45 T2T or nearly

T2T human Y chromosomes (Hallast et al. 2023) using MINIMAP2 (Li 2018) in splice-aware mode (-ax splice). Sequences of target regions were extracted using bamtobed (BEDTOOLS) (Quinlan and Hall 2010), translated into protein sequences, and searched against all known human proteins using BLASTP (Camacho et al. 2009) As a result, we identified sequences matching YAG proteins. The results of this analysis are summarized in Table S5.

Copy number estimation from short-read data in chimpanzee and gorilla. CUTADAPT (Martin 2011) was used to trim low-quality ends of reads (-q 20) and to trim Illumina TruSeq adaptors from short-read sequencing data analyzed in (Makova et al. 2024) (accession in Table S6). These pre-processed FASTQ files were mapped to either the gorilla or chimpanzee T2T reference genomes (versions GCF_029281585.2-RS_2024_02 and GCF_028858775.2-RS_2024_02, respectively) using BWA-MEM (Li 2013). AMPLICONE (Vegesna et al. 2019) was used to estimate copy numbers of YAG families for each individual. Gene definition files containing the genomic coordinates for each YAG gene copy in the reference ape genomes, as required by AMPLICONE, are provided in Table S15.

Analysis of significant changes in copy numbers along the phylogeny. CAFE (Mendes et al. 2021) was used to analyze the evolution of copy number within each YAG family along the phylogeny. We used median copy numbers for species with data for multiple individuals (human, chimpanzee, and gorilla; Tables S5 and S6). For CAFE, the Bonferroni-corrected significance threshold of $p = 0.05/13 = 0.0038$ (13 nodes in the tree) was used to identify significant changes in copy number across the phylogeny (Table S7).

Identification of palindromes and tandemly repeated arrays. Palindromic sequences (Table S16) were identified on the Y chromosome of each species using LASTZ (Harris, n.d.) self-alignments, followed by palindrome calling with PALINDROVER (Makova et al. 2024) with the following parameters: minimum arm length: 8 kb, minimum sequence identity: 98%, maximum spacer length: 500 kb. In human, a preprocessing step was applied to extract the euchromatic region of the Y chromosome by samtools faidx (Li et al. 2009), in order to exclude the highly repetitive heterochromatic region after coordinate 27,449,931 (Rhie et al. 2023). Candidate palindromes with ≥80% overlap with low-complexity sequences, simple repeats, or satellite DNA (based on REPEATMASKER (Smit, Hubley, and Green 2021) annotations) were excluded.

Tandemly repeated arrays on each Y chromosome were identified using AMPLICOVER v0.1.1-alpha (https://github.com/makovalab-psu/amplicover). AMPLICOVER detects tandemly repeated sequence copies (i.e., arrays) by identifying periodicity in the genomic distance between adjacent identical *k*-mers. Each chromosome was analyzed with *k*=21 and default parameters, via array signal calling, array boundary detection, and unit identification, as implemented in AMPLICOVER (Table S17).

Multiple sequence alignments. Multiple sequence alignments (MSAs) for phylogenetic and selection analyses were built from CDS sequences of all identified protein-coding copies of YAGs and their autosomal and X-chromosome homologs using MAFFT v7.526 (Katoh and Standley 2013) with the --globalpair and --maxiterate 1000 options, in a multi-step manner. For each YAG family, one MSA was built per species and an additional one for all non-Y homologs (if present). Next, for each gene family, all species-specific MSAs and non-Y homologs were combined into the final MSA using the --merge parameter. This approach was used for all genes except for *DAZ* and *RBMY*.

The *DAZ* gene contains an RRM domain (exons 2-6) and a 72-bp (or 90-bp) exon repeated multiple times (Fu et al. 2015), ranging from four copies in the Bornean orangutan to 16 in human (Fu et al. 2015). Variable numbers of *DAZ* repeats between individual gene copies make alignments of full CDSs challenging. Hence,

two MSAs were created for the *DAZ* gene family: one comprising all RRMs from all gene copies and another one comprising all short *DAZ* repeats from all gene copies.

The *RBMY* gene contains an internal repetitive region, SRGY (Ma et al. 1993; Elliott 2004), which complicates aligning coding sequences. To distinguish between repeat units across homologs, the full genomic sequences (exons and introns) of all *RBMY* homologs were aligned using `MAFFT` (Katoh and Standley 2013). With this approach, introns served as alignment anchors, simplifying the alignment process. The coding sequences of individual gene copies were then extracted. In the final MSA, we only considered exons annotated in all gene copies.

For all YAG families studied, final alignments were produced by trimming both ends of the MSAs, when needed, based on visual inspection. The 5' end was trimmed to the most common initiation codon and the 3' end was trimmed when it was substantially different among homologs.

Phylogenetic analysis. Maximum-likelihood phylogenies from the alignments for each gene family were inferred by `IQ-TREE` v2.3.6 (Minh et al. 2020) using automatic best-fit model selection with `MODELFINDER` (Kalyaanamoorthy et al. 2017). Branch support was assessed with 1,000 ultrafast bootstrap replicates.

RNA sequencing. Targeted (enriched with hybridization probes for YAGs) long-read Iso-Seq data for testis samples for six species (one sample per species, for all species studied but siamang) were from (Tomaszkiewicz et al. 2023), in which two technical replicates per sample were generated. Whole-genome long (PacBio) and short (Illumina) read expression data for the same testis samples from five non-human great ape species were from (Makova et al. 2024). For the human testis sample (A119, provided by the Cooperative Human Tissue Network (CHTN) under Penn State IRB STUDY00005084), targeted data were generated in (Tomaszkiewicz et al. 2023). Here, we generated an additional untargeted dataset from this sample. To do this, total RNA was isolated using the RNeasy Mini Kit (Qiagen, Germany) according to the manufacturer's instructions. Tissue was homogenized using a BeadBug 6 homogenizer (Benchmark Scientific, NJ, USA). RNA quantity and integrity were assessed using a TapeStation system (Agilent, CA, USA). For short-read RNA sequencing, libraries were prepared using the Illumina Stranded mRNA Library Prep kit and sequenced in paired-end mode (2×150 nt) on a NextSeq 2000 platform, resulting in 123.7 million read pairs. For long-read RNA sequencing, RNA libraries were generated using the Kinnex Full-Length RNA Kit based on the MAS-Seq method, according to the manufacturer's protocol. Sequencing was performed on a Sequel IIe system (Pacific Biosciences) using a single SMRT Cell, yielding 21.5 million reads.

Raw reads from both targeted and untargeted PacBio approaches were preprocessed using the Iso-Seq3 pipeline (PacBio) to produce full-length non-chimeric (FLNC) reads. For Illumina short-read RNA-seq, adapters were removed using `TRIMGALORE` (Krueger et al. 2023). Sample information and accession numbers are provided in Table S18.

Identification of YAG transcript reads in long-read data. PacBio FLNC reads were converted from `BAM` to `FASTA` format using `SAMTOOLS` (Danecek et al. 2021) and aligned to the corresponding species reference genome assemblies (listed above) in the splice-aware mode of `MINIMAP2` (Li 2018). Quality-trimmed Illumina reads, as described in the previous paragraph, were mapped to the corresponding reference genomes using `HISAT2` (Kim et al. 2019), and reads mapping to the Y chromosome were retained.

Transcriptome assembly and quality control. For each species, a T2T reference-informed transcriptome assembly was constructed using `STRINGTIE` (Shumate et al. 2022) in hybrid mode, integrating long and short reads. The three independently assembled transcript sets per species (two targeted—one per each technical

replicate—and one untargeted) were compared using GFFCOMPARE (Pertea and Pertea 2020). For each species, we identified a union of transcripts from these three sets, which was used in subsequent analyses. Transcripts were evaluated using SQANTI3 (Pardo-Palacios et al. 2024), and transcripts flagged as likely artifacts or degradation products were excluded.

Assignment of transcripts to YAG families. For each species, each transcript (represented as GFF coordinates) was assigned to a YAG family using one of two methods. In the first method, we searched for overlap between transcript coordinates and annotated YAG loci in the reference genomes using a custom script (annotation_based_on_region_intersection.R). If no overlap was found, we applied the second method. Here, we used transcript coordinates (in GFF format) to extract transcript sequences from the reference genome, using GFFREAD (Pertea and Pertea 2020). Next, we aligned the extracted sequences against a database of known YAG gene sequences we built from great ape T2T assembly annotations (extract_gene_families.py), using LASTZ (Harris, n.d.). These alignments were filtered to retain matches with ≥80% sequence identity over ≥100 bp, and used to assign the transcripts to YAG families.

ORF prediction. For all YAG transcripts identified in the previous step, ORFs were predicted in transcripts using GETORF from the EMBOSS suite (Rice, Longden, and Bleasby 2000), requiring a minimum size of 50 amino acids for the resulting protein. For additional validation, we used BLASTP (Camacho et al. 2009) to align the predicted ORF sequences against a reference database of great ape YAG proteins (create_protein_db.txt) that we constructed to include experimentally validated and predicted proteins for the seven YAG families, as available at NCBI.

Comparison of isoform structures. To identify alternative splicing patterns for each gene family, transcripts with ORFs were aligned to the longest human gene copy in each YAG family using ULTRA (Sahlin and Mäkinen 2021). This has allowed us to project all transcripts from the same family onto a common coordinate system. Structural isoforms were identified by converting alignments to the GFF format with BAMTOBED (Quinlan and Hall 2010), and comparing each transcript's exon-intron architecture against the full set using GFFCOMPARE (Pertea and Pertea 2020). Transcripts with identical exon-intron structure were assigned the same isoform identifier.

Identification of sequence isoforms from Iso-Seq reads. Transcript sequence diversity in YAG families was determined by identifying sequence-specific signatures. For this analysis, YAG-specific Iso-Seq reads were used (see the “Identification of YAG transcript reads in long-read data” section).

For each of *BPY2, CDY, HSFY, RBMY, TSPY,* and *VCY* gene families, first, gene-family-specific transcript reads were aligned to the longest copy for each gene family for each species using the splice-aware mode of MINIMAP2, to enable comparisons across all copies within a species. FREEBAYES (Garrison and Marth 2012) was used to perform variant calling on the alignments. Variants with transcript read depth greater than 30× were used in the signature analysis. Variable positions among reference gene copies were also noted. Second, each transcript read was processed to determine whether a variant was present or absent at positions defined in the previous step. The combination of variants specified a transcript sequence signature, or a fingerprint. The results of this analysis were compiled into count tables summarizing the frequency distributions of signatures across samples (Additional Data File 6). Third, for these transcripts, which now have assigned sequence signatures, we identified splicing patterns and matched them to structural isoforms as defined in “Comparison of isoform structures”. To do this, transcript reads (with signatures) from each species were mapped to the corresponding T2T reference genome assemblies using MINIMAP2 (Li 2018). As a result of this step, each transcript read had a previously assigned structural identifier. Summarizing these results, we built tables with rows representing sequence signatures and columns representing transcript structural isoforms

(Additional Data File 1). Finally, we filtered and translated the observed transcript isoforms sequences into protein isoforms using the following three steps. First, a transcript isoform was considered only if it was represented by at least 2% of the total number of full-length reads identified for the given gene family within a species, or by at least five reads, whichever was higher. Second, we required that each transcript isoform be supported by at least two of the three independently assembled transcript sets (see section "Transcriptome assembly and quality control"). Third, to exclude sequencing errors, reads representing each retained transcript isoform were collected, and their consensus sequences were called using `SPOA` (Vaser et al. 2017). An ORF within each transcript isoform was identified with `ORF-FINDER` (Rombel et al. 2002). Finally, the retrieved ORFs were translated using the `BIOPYTHON` (Cock et al. 2009) library, using the default codon table—NCBI Genetic Code Table 1 (https://www.ncbi.nlm.nih.gov/Taxonomy/Utils/wprintgc.cgi).

For the *DAZ* gene family, first, transcript reads containing at least part of the RRM domain were identified. Given the composition of *DAZ* genes 5'$(RRM)_N$(DAZ repeat)$_M$3', where N is the number of RRMs (N=1-3) and M is the number of *DAZ* repeats, and considering reads are sequences from the poly A tail (3' -> 5'), this ensures that the retained reads contain the full sequence of *DAZ* repeats. Second, for each species, all *DAZ* repeat sequences were collected, and an MSA of just these sequences was produced using `MAFFT` (Katoh and Standley 2013) in global alignment mode. Third, `HMMBUILD` (`HMMER` 3.4, (Eddy 2011)) was used to create the Hidden Markov Model (`HMM`) profile of *DAZ* repeats. Fourth, utilizing this `HMM` profile, `HMMSEARCH` (`HMMER` 3.4, (Eddy 2011)) was used to identify individual *DAZ* repeats in each read. Fifth, unique *DAZ* repeat sequences occurring within each species were collected and sorted by the number of occurrences (Additional Data File 2). The sorted list of identified *DAZ* repeats (Additional Data File 2) contains a small number of high-abundance *DAZ* repeat sequences and a long list of low-abundance sequences. For each species, the top N most abundant sequences were considered true repeat sequences. N was manually set for each species after visual inspection of the count tables (Additional Data File 2) (to identify a natural breakpoint in abundance between signal and noise) as follows: 10 for human and gorilla, 20 for bonobo and chimpanzee, 10 for Bornean orangutan, and 3 for Sumatran orangutan. The 'true' (i.e., high-abundance repeat sequences) were labeled A, B, C, etc. The remaining low-abundance sequences in the count tables received the label of the closest (according to the Hamming distance) true repeat sequence. Sixth, a signature consisting of a pattern of *DAZ* repeat labels based on the repeat content was constructed for each read. Seventh, a consensus sequence was called from reads clustered by their *DAZ* repeat content signatures using `SPOA` (Vaser et al. 2017), and a protein sequence was extracted from an open reading frame identified by `ORF-FINDER` (Rombel et al. 2002). The scripts for variant calling, signature extraction, mapping, splice pattern matching, alignment, HMM, and consensus calling scripts are available on GitHub (https://github.com/makovalab-psu/YAGs-survival).

Comparison of reference-augmented structural isoforms with a set of previous *de novo* assembled structural isoforms. For this comparison, we used transcripts from the section "Identification of sequence isoforms from Iso-Seq reads.") from Table S13. Here, we identified 182 replicate-supported transcripts, whereas in (Tomaszkiewicz et al. 2023)we identified 1,510 transcripts. On average, transcripts identified by (Tomaszkiewicz et al. 2023) were shorter (mean length of 820 bp in (Tomaszkiewicz et al. 2023), as compared to those in our reference-based approach (mean length = 1,215 bp). Considering our approach filters reads based on read length a more fair comparison of methods is provided in (Note S3).

RNA-seq expression quantification. Expression of YAG transcripts was quantified from testis short RNA-seq reads generated in (Makova et al. 2024) (Table S18) using `SALMON` v1.10.3 (Patro et al. 2017). To assess the effect of using a genome reference on YAG expression estimates, two transcriptomes were constructed per species. The first transcriptome consisted of the NCBI RefSeq gene annotations. The second, reference-augmented transcriptome was constructed by adding species-specific novel YAG transcript

sequences (which we identified by incorporating T2T reference genome assemblies into analysis, see sections "Identification of YAG transcript reads from long-read data" through "Identification of sequence isoforms from IsoSeq reads.") to the standard RefSeq reference. `SALMON` indices were built with a *k*-mer size of 31. Quantification was performed using selective alignment (`--validateMappings`), correcting for sequence-specific biases (`--seqBias`), and fragment-level GC biases (`--gcBias`). Expression differences between standard and reference-augmented transcriptomes were reported in read counts and in TPM. Fold differences were computed as log2((augmented + 1) / (standard + 1)), with a pseudocount of 1 to handle zero counts, and are reported in Table S10.

Protein folding predictions and clustering. All transcripts from the previous step that had an ORF were utilized for protein structure prediction, which was used in the following steps. First, by collapsing transcripts differing by synonymous variants, we identified and included only unique predicted protein isoforms. Second, `COLABFOLD` v1.5.5 (Mirdita et al. 2022) was run to produce structure predictions, MSAs of related proteins, and AlphaFold2 structure prediction confidence measures (pLDDT). Third, the predicted protein structures were clustered using `FOLDSEEK` commit 10.941cd33 (van Kempen et al. 2024) with default parameters.

Selection analysis. All alignments from the "Multiple sequence alignments" step were examined for the presence of premature stop codons and the presence of identical gene copies—only unique copies were retained, using `HYPHY cln` (Kosakovsky Pond et al. 2020). For each gene family, the alignment and the phylogenetic trees (from the "Phylogenetic analysis" step above) were fitted to the standard MG94 (Muse and Gaut 1994) model to estimate a mean *dN*/*dS* and its confidence intervals using `HYPHY`. BUSTED-E within `HYPHY` was used to detect episodic diversifying selection and to identify errors caused by misalignments. Each gene family was tested with the following tests:

1. Mean *dN*/*dS* ≠ 1: a likelihood ratio test under the MG94 global model.
2. Branch heterogeneity: a test for variation in selection pressure across branches, via fitting of a local MG94 model (separate *dN*/*dS* for each branch) and comparing it to the global MG94 model (single *dN/dS* across the phylogeny) using a Likelihood Ratio Test.
3. BUSTED-E: a gene-wide test for episodic diversifying selection that also estimates whether or not there is a non-zero error component.
4. aBSREL-selected branches: a test for evidence of episodic diversifying selection on individual branches.
5. MEME-selected sites: a test of episodic diversifying selection on individual sites.

Assessment of functional impact of non-synonymous substitutions. For each gene, a consensus protein sequence was derived from an MSA of coding sequences across species (see section "**Multiple sequence alignments.**"**)**. Protein sequence and substitutions of interest were submitted to the `SIFT` web server (sift.bii.a-star.edu.sg, Sim et al. 2012). `SIFT` (Kumar, Henikoff, and Ng 2009) predictions and confidence scores were retrieved from the server output and formatted into a table format. Substitutions were classified as "Affect Protein Function" (score < 0.05) or "Tolerated" (score ≥ 0.05). Some predictions were flagged as low confidence (insufficient sequence diversity). All code used for processing of `SIFT` results is available at https://github.com/makovalab-psu/YAGs-survival/tree/main/SIFT_annotation.

Acknowledgements

We would like to thank Françoise Thibaud-Nissen, Kelly McGarvey, and Shashikant Pujar of the NCBI gene annotation team for feedback, assistance, and review during gene curation. We would like to thank Linnéa Smeds for careful reading of the manuscript and helpful comments. The research in KDM's laboratory is supported by the grant R35GM151945 from the NIH and by the Willaman Chair Endowment Fund from the Eberly College of Science to KDM. Computations were performed at the Penn State Institute of Computational Data Sciences (RRID:SCR_025154), which provided access to computational research infrastructure within the Roar Core Facility (RRID:SCR_026424).

References

Andrés, Olga, Thomas Kellermann, Francesc López-Giráldez, Julio Rozas, Xavier Domingo-Roura, and Montserrat Bosch. 2008. “RPS4Y Gene Family Evolution in Primates.” *BMC Evolutionary Biology* 8 (1): 142.

Assis, Raquel, and Doris Bachtrog. 2013. “Neofunctionalization of Young Duplicate Genes in *Drosophila*.” *Proceedings of the National Academy of Sciences of the United States of America* 110 (43): 17409–14.

Bergeron, Lucie A., Søren Besenbacher, Jiao Zheng, Panyi Li, Mads Frost Bertelsen, Benoit Quintard, Joseph I. Hoffman, Zhipeng Li, Judy St Leger, Changwei Shao, Josefin Stiller, M. Thomas P. Gilbert, Mikkel H. Schierup, and Guojie Zhang. 2023. “Evolution of the Germline Mutation Rate across Vertebrates.” *Nature* 615 (7951): 285–91.

Betrán, Esther, Jeffery P. Demuth, and Anna Williford. 2012. “Why Chromosome Palindromes?” *International Journal of Evolutionary Biology* 2012 (July):207958.

Bhowmick, Bejon Kumar, Yoko Satta, and Naoyuki Takahata. 2007. “The Origin and Evolution of Human Ampliconic Gene Families and Ampliconic Structure.” *Genome Research* 17 (4): 441–50.

Bielawski, J. P., and Z. Yang. 2001. “Positive and Negative Selection in the DAZ Gene Family.” *Molecular Biology and Evolution* 18 (4): 523–29.

Brashear, Wesley A., Terje Raudsepp, and William J. Murphy. 2018. “Evolutionary Conservation of Y Chromosome Ampliconic Gene Families despite Extensive Structural Variation.” *Genome Research* 28 (12): 1841–51.

Camacho, Christiam, George Coulouris, Vahram Avagyan, Ning Ma, Jason Papadopoulos, Kevin Bealer, and Thomas L. Madden. 2009. “BLAST+: Architecture and Applications.” *BMC Bioinformatics* 10 (1): 421.

Cao, Peng-Rong, Lei Wang, Yu-Chao Jiang, Yin-Sha Yi, Fang Qu, Tao-Cheng Liu, and Yuan Lv. 2015. “De Novo Origin of VCY2 from Autosome to Y-Transposed Amplicon.” *PloS One* 10 (3): e0119651.

Cechova, Monika, Rahulsimham Vegesna, Marta Tomaszkiewicz, Robert S. Harris, Di Chen, Samarth Rangavittal, Paul Medvedev, and Kateryna D. Makova. 2020. “Dynamic Evolution of Great Ape Y Chromosomes.” *Proceedings of the National Academy of Sciences of the United States of America* 117 (42): 26273–80.

Charlesworth, Brian. 2003. “The Organization and Evolution of the Human Y Chromosome.” *Genome Biology* 4 (9): 226.

Choi, Jin, Eitetsu Koh, Hiromi Suzuki, Yuji Maeda, Atsumi Yoshida, and Mikio Namiki. 2007. “Alu Sequence Variants of the BPY2 Gene in Proven Fertile and Infertile Men with Sertoli Cell-Only Phenotype: Alu Sequence Variants of BPY2.” *International Journal of Urology: Official Journal of the Japanese Urological Association* 14 (5): 431–35.

Cock, Peter J. A., Tiago Antao, Jeffrey T. Chang, Brad A. Chapman, Cymon J. Cox, Andrew Dalke, Iddo Friedberg, Thomas Hamelryck, Frank Kauff, Bartek Wilczynski, and Michiel J. L. de Hoon. 2009. “Biopython: Freely Available Python Tools for Computational Molecular Biology and Bioinformatics.” *Bioinformatics (Oxford, England)* 25 (11): 1422–23.

Colaco, Stacy, and Deepak Modi. 2018. “Genetics of the Human Y Chromosome and Its Association with Male Infertility.” *Reproductive Biology and Endocrinology: RB&E* 16 (1): 14.

Connallon, Tim, and Andrew G. Clark. 2010. “Gene Duplication, Gene Conversion and the Evolution of the Y Chromosome.” *Genetics* 186 (1): 277–86.

Danecek, Petr, James K. Bonfield, Jennifer Liddle, John Marshall, Valeriu Ohan, Martin O. Pollard, Andrew Whitwham, Thomas Keane, Shane A. McCarthy, Robert M. Davies, and Heng Li. 2021. “Twelve Years of SAMtools and BCFtools.” *GigaScience* 10 (2). https://doi.org/10.1093/gigascience/giab008.

Davis, Jamie K., Pamela J. Thomas, NISC Comparative Sequencing Program, and James W. Thomas. 2010. “A W-Linked Palindrome and Gene Conversion in New World Sparrows and Blackbirds.” *Chromosome Research: An International Journal on the Molecular, Supramolecular and Evolutionary Aspects of Chromosome Biology* 18 (5): 543–53.

Delbridge, Margaret L., Guy Longepied, Danielle Depetris, Marie-Genevieve Mattei, Christine M. Disteche, Jennifer A. Marshall Graves, and Michael J. Mitchell. 2004. “TSPY, the Candidate Gonadoblastoma Gene on the Human Y Chromosome, Has a Widely Expressed Homologue on the X - Implications for Y Chromosome Evolution.” *Chromosome Research: An International Journal on the Molecular, Supramolecular and Evolutionary Aspects of Chromosome Biology* 12 (4): 345–56.

Dorus, Steve, Sandra L. Gilbert, Michele L. Forster, Robert J. Barndt, and Bruce T. Lahn. 2003. “The

CDY-Related Gene Family: Coordinated Evolution in Copy Number, Expression Profile and Protein Sequence." *Human Molecular Genetics* 12 (14): 1643–50.
Eddy, Sean R. 2011. "Accelerated Profile HMM Searches." *PLoS Computational Biology* 7 (10): e1002195.
Elliott, David J. 2004. "The Role of Potential Splicing Factors Including RBMY, RBMX, hnRNPG-T and STAR Proteins in Spermatogenesis." *International Journal of Andrology* 27 (6): 328–34.
Elliott, David J., Caroline Dalgliesh, Gerald Hysenaj, and Ingrid Ehrmann. 2019. "RBMX Family Proteins Connect the Fields of Nuclear RNA Processing, Disease and Sex Chromosome Biology." *The International Journal of Biochemistry & Cell Biology* 108 (March):1–6.
Fu, Xia-Fei, Shun-Feng Cheng, Lin-Qing Wang, Shen Yin, Massimo De Felici, and Wei Shen. 2015. "DAZ Family Proteins, Key Players for Germ Cell Development." *International Journal of Biological Sciences* 11 (10): 1226–35.
Garrison, Erik, and Gabor Marth. 2012. "Haplotype-Based Variant Detection from Short-Read Sequencing." *arXiv [q-bio.GN]*. https://doi.org/10.48550/ARXIV.1207.3907.
Geraldes, Armando, Teri Rambo, Rod A. Wing, Nuno Ferrand, and Michael W. Nachman. 2010. "Extensive Gene Conversion Drives the Concerted Evolution of Paralogous Copies of the SRY Gene in European Rabbits." *Molecular Biology and Evolution* 27 (11): 2437–40.
Ghenu, Ana-Hermina, Benjamin M. Bolker, Don J. Melnick, and Ben J. Evans. 2016. "Multicopy Gene Family Evolution on Primate Y Chromosomes." *BMC Genomics* 17 (1): 157.
Goldfarb, Tamara, Vamsi K. Kodali, Shashikant Pujar, Vyacheslav Brover, Barbara Robbertse, Catherine M. Farrell, Dong-Ha Oh, Alexander Astashyn, Olga Ermolaeva, Diana Haddad, Wratko Hlavina, Jinna Hoffman, John D. Jackson, Vinita S. Joardar, David Kristensen, Patrick Masterson, Kelly M. McGarvey, Richard McVeigh, Eyal Mozes, Michael R. Murphy, Susan S. Schafer, Alexander Souvorov, Brett Spurrier, Pooja K. Strope, Hanzhen Sun, Anjana R. Vatsan, Craig Wallin, David Webb, J. Rodney Brister, Eneida Hatcher, Avi Kimchi, William Klimke, Aron Marchler-Bauer, Kim D. Pruitt, Françoise Thibaud-Nissen, and Terence D. Murphy. 2025. "NCBI RefSeq: Reference Sequence Standards through 25 Years of Curation and Annotation." *Nucleic Acids Research* 53 (D1): D243–57.
Grondin, K., B. Papadopoulou, and M. Ouellette. 1993. "Homologous Recombination between Direct Repeat Sequences Yields P-Glycoprotein Containing Amplicons in Arsenite Resistant Leishmania." *Nucleic Acids Research* 21 (8): 1895–1901.
Hallast, Pille, Patricia Balaresque, Georgina R. Bowden, Stéphane Ballereau, and Mark A. Jobling. 2013. "Recombination Dynamics of a Human Y-Chromosomal Palindrome: Rapid GC-Biased Gene Conversion, Multi-Kilobase Conversion Tracts, and Rare Inversions." *PLoS Genetics* 9 (7): e1003666.
Hallast, Pille, Peter Ebert, Mark Loftus, Feyza Yilmaz, Peter A. Audano, Glennis A. Logsdon, Marc Jan Bonder, Weichen Zhou, Wolfram Höps, Kwondo Kim, Chong Li, Savannah J. Hoyt, Philip C. Dishuck, David Porubsky, Fotios Tsetsos, Jee Young Kwon, Qihui Zhu, Katherine M. Munson, Patrick Hasenfeld, William T. Harvey, Alexandra P. Lewis, Jennifer Kordosky, Kendra Hoekzema, Human Genome Structural Variation Consortium (HGSVC), Rachel J. O'Neill, Jan O. Korbel, Chris Tyler-Smith, Evan E. Eichler, Xinghua Shi, Christine R. Beck, Tobias Marschall, Miriam K. Konkel, and Charles Lee. 2023. "Assembly of 43 Human Y Chromosomes Reveals Extensive Complexity and Variation." *Nature* 621 (7978): 355–64.
Harris, Bob. n.d. *Lastz: Program for Aligning DNA Sequences, a Pairwise Aligner*. Github. Accessed December 12, 2024. https://github.com/lastz/lastz.
Hobza, Roman, Martina Lengerova, Julia Svoboda, Hana Kubekova, Eduard Kejnovsky, and Boris Vyskot. 2006. "An Accumulation of Tandem DNA Repeats on the Y Chromosome in Silene Latifolia during Early Stages of Sex Chromosome Evolution." *Chromosoma* 115 (5): 376–82.
Huang, Zhen, Zaoxu Xu, Hao Bai, Yongji Huang, Na Kang, Xiaoting Ding, Jing Liu, Haoran Luo, Chentao Yang, Wanjun Chen, Qixin Guo, Lingzhan Xue, Xueping Zhang, Li Xu, Meiling Chen, Honggao Fu, Youling Chen, Zhicao Yue, Tatsuo Fukagawa, Shanlin Liu, Guobin Chang, and Luohao Xu. 2023. "Evolutionary Analysis of a Complete Chicken Genome." *Proceedings of the National Academy of Sciences of the United States of America* 120 (8): e2216641120.
Hughes, Jennifer F., Helen Skaletsky, and David C. Page. 2012. "Sequencing of Rhesus Macaque Y Chromosome Clarifies Origins and Evolution of the DAZ (Deleted in AZoospermia) Genes." *BioEssays: News and Reviews in Molecular, Cellular and Developmental Biology* 34 (12): 1035–44.
Hughes, Jennifer F., Helen Skaletsky, Tatyana Pyntikova, Natalia Koutseva, Terje Raudsepp, Laura G. Brown, Daniel W. Bellott, Ting-Jan Cho, Shannon Dugan-Rocha, Ziad Khan, Colin Kremitzki, Catrina Fronick, Tina A. Graves-Lindsay, Lucinda Fulton, Wesley C. Warren, Richard K. Wilson, Elaine Owens, James E.

Womack, William J. Murphy, Donna M. Muzny, Kim C. Worley, Bhanu P. Chowdhary, Richard A. Gibbs, and David C. Page. 2020. “Sequence Analysis in Bos Taurus Reveals Pervasiveness of X-Y Arms Races in Mammalian Lineages.” *Genome Research* 30 (12): 1716–26.

Iñiguez, Luis P., and Georgina Hernández. 2017. “The Evolutionary Relationship between Alternative Splicing and Gene Duplication.” *Frontiers in Genetics* 8 (February):14.

Iwase, Mineyo, Yoko Satta, Hirohisa Hirai, Yuriko Hirai, and Naoyuki Takahata. 2010. “Frequent Gene Conversion Events between the X and Y Homologous Chromosomal Regions in Primates.” *BMC Evolutionary Biology* 10 (July):225.

Jumper, John, Richard Evans, Alexander Pritzel, Tim Green, Michael Figurnov, Olaf Ronneberger, Kathryn Tunyasuvunakool, Russ Bates, Augustin Žídek, Anna Potapenko, Alex Bridgland, Clemens Meyer, Simon A. A. Kohl, Andrew J. Ballard, Andrew Cowie, Bernardino Romera-Paredes, Stanislav Nikolov, Rishub Jain, Jonas Adler, Trevor Back, Stig Petersen, David Reiman, Ellen Clancy, Michal Zielinski, Martin Steinegger, Michalina Pacholska, Tamas Berghammer, Sebastian Bodenstein, David Silver, Oriol Vinyals, Andrew W. Senior, Koray Kavukcuoglu, Pushmeet Kohli, and Demis Hassabis. 2021. “Highly Accurate Protein Structure Prediction with AlphaFold.” *Nature* 596 (7873): 583–89.

Kalyaanamoorthy, Subha, Bui Quang Minh, Thomas K. F. Wong, Arndt von Haeseler, and Lars S. Jermiin. 2017. “ModelFinder: Fast Model Selection for Accurate Phylogenetic Estimates.” *Nature Methods* 14 (6): 587–89.

Katoh, Kazutaka, and Daron M. Standley. 2013. “MAFFT Multiple Sequence Alignment Software Version 7: Improvements in Performance and Usability.” *Molecular Biology and Evolution* 30 (4): 772–80.

Kempen, Michel van, Stephanie S. Kim, Charlotte Tumescheit, Milot Mirdita, Jeongjae Lee, Cameron L. M. Gilchrist, Johannes Söding, and Martin Steinegger. 2024. “Fast and Accurate Protein Structure Search with Foldseek.” *Nature Biotechnology* 42 (2): 243–46.

Kim, Daehwan, Joseph M. Paggi, Chanhee Park, Christopher Bennett, and Steven L. Salzberg. 2019. “Graph-Based Genome Alignment and Genotyping with HISAT2 and HISAT-Genotype.” *Nature Biotechnology* 37 (8): 907–15.

Kosakovsky Pond, Sergei L., Art F. Y. Poon, Ryan Velazquez, Steven Weaver, N. Lance Hepler, Ben Murrell, Stephen D. Shank, Brittany Rife Magalis, Dave Bouvier, Anton Nekrutenko, Sadie Wisotsky, Stephanie J. Spielman, Simon D. W. Frost, and Spencer V. Muse. 2020. “HyPhy 2.5-A Customizable Platform for Evolutionary Hypothesis Testing Using PHYlogenies.” *Molecular Biology and Evolution* 37 (1): 295–99.

Krausz, Csilla, and Chiara Abrardo. 2025. “The Y Chromosome: Male Reproduction and beyond.” *Fertility and Sterility* 123 (6): 921–32.

Krueger, Felix, Frankie James, Phil Ewels, Ebrahim Afyounian, Michael Weinstein, Benjamin Schuster-Boeckler, Gert Hulselmans, and sclamons. 2023. *FelixKrueger/TrimGalore: v0.6.10 - Add Default Decompression Path*. Zenodo. https://doi.org/10.5281/ZENODO.7598955.

Kumar, Prateek, Steven Henikoff, and Pauline C. Ng. 2009. “Predicting the Effects of Coding Non-Synonymous Variants on Protein Function Using the SIFT Algorithm.” *Nature Protocols* 4 (7): 1073–81.

Lahn, B. T., and D. C. Page. 1997. “Functional Coherence of the Human Y Chromosome.” *Science (New York, N.Y.)* 278 (5338): 675–80.

———. 1999. “Retroposition of Autosomal mRNA Yielded Testis-Specific Gene Family on Human Y Chromosome.” *Nature Genetics* 21 (4): 429–33.

Leung, Szi Kay, Aaron R. Jeffries, Isabel Castanho, Ben T. Jordan, Karen Moore, Jonathan P. Davies, Emma L. Dempster, Nicholas J. Bray, Paul O’Neill, Elizabeth Tseng, Zeshan Ahmed, David A. Collier, Erin D. Jeffery, Shyam Prabhakar, Leonard Schalkwyk, Connor Jops, Michael J. Gandal, Gloria M. Sheynkman, Eilis Hannon, and Jonathan Mill. 2021. “Full-Length Transcript Sequencing of Human and Mouse Cerebral Cortex Identifies Widespread Isoform Diversity and Alternative Splicing.” *Cell Reports* 37 (7): 110022.

Li, Heng. 2018. “Minimap2: Pairwise Alignment for Nucleotide Sequences.” *Bioinformatics (Oxford, England)* 34 (18): 3094–3100.

Li, Heng, Bob Handsaker, Alec Wysoker, Tim Fennell, Jue Ruan, Nils Homer, Gabor Marth, Goncalo Abecasis, Richard Durbin, and 1000 Genome Project Data Processing Subgroup. 2009. “The Sequence Alignment/Map Format and SAMtools.” *Bioinformatics (Oxford, England)* 25 (16): 2078–79.

Lingenfelter, P. A., M. L. Delbridge, S. Thomas, H. E. Hoekstra, M. J. Mitchell, J. A. Graves, and C. M. Disteche. 2001. “Expression and Conservation of Processed Copies of the RBMX Gene.” *Mammalian Genome: Official Journal of the International Mammalian Genome Society* 12 (7): 538–45.

Lucotte, Elise A., Valdís Björt Guðmundsdóttir, Jacob M. Jensen, Laurits Skov, Moisès Coll Macià, Kristian

Almstrup, Mikkel H. Schierup, Agnar Helgason, and Kari Stefansson. 2023. “Characterizing the Evolution and Phenotypic Impact of Ampliconic Y Chromosome Regions.” *Nature Communications* 14 (1): 3990.
Lucotte, Elise A., Laurits Skov, Jacob Malte Jensen, Moisès Coll Macià, Kasper Munch, and Mikkel H. Schierup. 2018. “Dynamic Copy Number Evolution of X- and Y-Linked Ampliconic Genes in Human Populations.” *Genetics* 209 (3): 907–20.
Ma, K., J. D. Inglis, A. Sharkey, W. A. Bickmore, R. E. Hill, E. J. Prosser, R. M. Speed, E. J. Thomson, M. Jobling, and K. Taylor. 1993. “A Y Chromosome Gene Family with RNA-Binding Protein Homology: Candidates for the Azoospermia Factor AZF Controlling Human Spermatogenesis.” *Cell* 75 (7): 1287–95.
Makova, Kateryna D., and Wen-Hsiung Li. 2002. “Strong Male-Driven Evolution of DNA Sequences in Humans and Apes.” *Nature* 416 (6881): 624–26.
Makova, Kateryna D., Brandon D. Pickett, Robert S. Harris, Gabrielle A. Hartley, Monika Cechova, Karol Pal, Sergey Nurk, Dongahn Yoo, Qiuhui Li, Prajna Hebbar, Barbara C. McGrath, Francesca Antonacci, Margaux Aubel, Arjun Biddanda, Matthew Borchers, Erich Bornberg-Bauer, Gerard G. Bouffard, Shelise Y. Brooks, Lucia Carbone, Laura Carrel, Andrew Carroll, Pi-Chuan Chang, Chen-Shan Chin, Daniel E. Cook, Sarah J. C. Craig, Luciana de Gennaro, Mark Diekhans, Amalia Dutra, Gage H. Garcia, Patrick G. S. Grady, Richard E. Green, Diana Haddad, Pille Hallast, William T. Harvey, Glenn Hickey, David A. Hillis, Savannah J. Hoyt, Hyeonsoo Jeong, Kaivan Kamali, Sergei L. Kosakovsky Pond, Troy M. LaPolice, Charles Lee, Alexandra P. Lewis, Yong-Hwee E. Loh, Patrick Masterson, Kelly M. McGarvey, Rajiv C. McCoy, Paul Medvedev, Karen H. Miga, Katherine M. Munson, Evgenia Pak, Benedict Paten, Brendan J. Pinto, Tamara Potapova, Arang Rhie, Joana L. Rocha, Fedor Ryabov, Oliver A. Ryder, Samuel Sacco, Kishwar Shafin, Valery A. Shepelev, Viviane Slon, Steven J. Solar, Jessica M. Storer, Peter H. Sudmant, Sweetalana, Alex Sweeten, Michael G. Tassia, Françoise Thibaud-Nissen, Mario Ventura, Melissa A. Wilson, Alice C. Young, Huiqing Zeng, Xinru Zhang, Zachary A. Szpiech, Christian D. Huber, Jennifer L. Gerton, Soojin V. Yi, Michael C. Schatz, Ivan A. Alexandrov, Sergey Koren, Rachel J. O’Neill, Evan E. Eichler, and Adam M. Phillippy. 2024. “The Complete Sequence and Comparative Analysis of Ape Sex Chromosomes.” *Nature* 630 (8016): 401–11.
Manz, E., F. Schnieders, A. M. Brechlin, and J. Schmidtke. 1993. “TSPY-Related Sequences Represent a Microheterogeneous Gene Family Organized as Constitutive Elements in DYZ5 Tandem Repeat Units on the Human Y Chromosome.” *Genomics* 17 (3): 726–31.
Marais, Gabriel A. B., Paulo R. A. Campos, and Isabel Gordo. 2010. “Can Intra-Y Gene Conversion Oppose the Degeneration of the Human Y Chromosome? A Simulation Study.” *Genome Biology and Evolution* 2 (0): 347–57.
Martí, Emiliano, and Amanda M. Larracuente. 2023. “Genetic Conflict and the Origin of Multigene Families: Implications for Sex Chromosome Evolution.” *Proceedings. Biological Sciences* 290 (2010): 20231823.
Martin, Marcel. 2011. “Cutadapt Removes Adapter Sequences from High-Throughput Sequencing Reads.” *EMBnet.journal* 17 (1): 10.
Mendes, Fábio K., Dan Vanderpool, Ben Fulton, and Matthew W. Hahn. 2021. “CAFE 5 Models Variation in Evolutionary Rates among Gene Families.” *Bioinformatics (Oxford, England)* 36 (22-23): 5516–18.
Minh, Bui Quang, Heiko A. Schmidt, Olga Chernomor, Dominik Schrempf, Michael D. Woodhams, Arndt von Haeseler, and Robert Lanfear. 2020. “IQ-TREE 2: New Models and Efficient Methods for Phylogenetic Inference in the Genomic Era.” *Molecular Biology and Evolution* 37 (5): 1530–34.
Mirdita, Milot, Konstantin Schütze, Yoshitaka Moriwaki, Lim Heo, Sergey Ovchinnikov, and Martin Steinegger. 2022. “ColabFold: Making Protein Folding Accessible to All.” *Nature Methods* 19 (6): 679–82.
Murrell, Ben, Joel O. Wertheim, Sasha Moola, Thomas Weighill, Konrad Scheffler, and Sergei L. Kosakovsky Pond. 2012. “Detecting Individual Sites Subject to Episodic Diversifying Selection.” *PLoS Genetics* 8 (7): e1002764.
Muse, S. V., and B. S. Gaut. 1994. “A Likelihood Approach for Comparing Synonymous and Nonsynonymous Nucleotide Substitution Rates, with Application to the Chloroplast Genome.” *Molecular Biology and Evolution* 11 (5): 715–24.
Ohta, T. 1989. “The Mutational Load of a Multigene Family with Uniform Members.” *Genetical Research* 53 (2): 141–45.
Olagunju, Temitayo A., Benjamin D. Rosen, Holly L. Neibergs, Gabrielle M. Becker, Kimberly M. Davenport, Christine G. Elsik, Tracy S. Hadfield, Sergey Koren, Kristen L. Kuhn, Arang Rhie, Katie A. Shira, Amy L. Skibiel, Morgan R. Stegemiller, Jacob W. Thorne, Patricia Villamediana, Noelle E. Cockett, Brenda M. Murdoch, and Timothy P. L. Smith. 2024. “Telomere-to-Telomere Assemblies of Cattle and Sheep

Y-Chromosomes Uncover Divergent Structure and Gene Content." *Nature Communications* 15 (1): 8277.
Pardo-Palacios, Francisco J., Angeles Arzalluz-Luque, Liudmyla Kondratova, Pedro Salguero, Jorge Mestre-Tomás, Rocío Amorín, Eva Estevan-Morió, Tianyuan Liu, Adalena Nanni, Lauren McIntyre, Elizabeth Tseng, and Ana Conesa. 2024. "SQANTI3: Curation of Long-Read Transcriptomes for Accurate Identification of Known and Novel Isoforms." *Nature Methods* 21 (5): 793–97.
Patro, Rob, Geet Duggal, Michael I. Love, Rafael A. Irizarry, and Carl Kingsford. 2017. "Salmon Provides Fast and Bias-Aware Quantification of Transcript Expression." *Nature Methods* 14 (4): 417–19.
Pertea, Geo, and Mihaela Pertea. 2020. "GFF Utilities: GffRead and GffCompare." *F1000Research* 9 (304): 304.
Quinlan, Aaron R., and Ira M. Hall. 2010. "BEDTools: A Flexible Suite of Utilities for Comparing Genomic Features." *Bioinformatics (Oxford, England)* 26 (6): 841–42.
Rhie, Arang, Sergey Nurk, Monika Cechova, Savannah J. Hoyt, Dylan J. Taylor, Nicolas Altemose, Paul W. Hook, Sergey Koren, Mikko Rautiainen, Ivan A. Alexandrov, Jamie Allen, Mobin Asri, Andrey V. Bzikadze, Nae-Chyun Chen, Chen-Shan Chin, Mark Diekhans, Paul Flicek, Giulio Formenti, Arkarachai Fungtammasan, Carlos Garcia Giron, Erik Garrison, Ariel Gershman, Jennifer L. Gerton, Patrick G. S. Grady, Andrea Guarracino, Leanne Haggerty, Reza Halabian, Nancy F. Hansen, Robert Harris, Gabrielle A. Hartley, William T. Harvey, Marina Haukness, Jakob Heinz, Thibaut Hourlier, Robert M. Hubley, Sarah E. Hunt, Stephen Hwang, Miten Jain, Rupesh K. Kesharwani, Alexandra P. Lewis, Heng Li, Glennis A. Logsdon, Julian K. Lucas, Wojciech Makalowski, Christopher Markovic, Fergal J. Martin, Ann M. Mc Cartney, Rajiv C. McCoy, Jennifer McDaniel, Brandy M. McNulty, Paul Medvedev, Alla Mikheenko, Katherine M. Munson, Terence D. Murphy, Hugh E. Olsen, Nathan D. Olson, Luis F. Paulin, David Porubsky, Tamara Potapova, Fedor Ryabov, Steven L. Salzberg, Michael E. G. Sauria, Fritz J. Sedlazeck, Kishwar Shafin, Valery A. Shepelev, Alaina Shumate, Jessica M. Storer, Likhitha Surapaneni, Angela M. Taravella Oill, Françoise Thibaud-Nissen, Winston Timp, Marta Tomaszkiewicz, Mitchell R. Vollger, Brian P. Walenz, Allison C. Watwood, Matthias H. Weissensteiner, Aaron M. Wenger, Melissa A. Wilson, Samantha Zarate, Yiming Zhu, Justin M. Zook, Evan E. Eichler, Rachel J. O'Neill, Michael C. Schatz, Karen H. Miga, Kateryna D. Makova, and Adam M. Phillippy. 2023. "The Complete Sequence of a Human Y Chromosome." *Nature* 621 (7978): 344–54.
Rice, P., I. Longden, and A. Bleasby. 2000. "EMBOSS: The European Molecular Biology Open Software Suite." *Trends in Genetics: TIG* 16 (6): 276–77.
Rombel, Irene T., Kathryn F. Sykes, Simon Rayner, and Stephen Albert Johnston. 2002. "ORF-FINDER: A Vector for High-Throughput Gene Identification." *Gene* 282 (1-2): 33–41.
Rozen, Steve, Helen Skaletsky, Janet D. Marszalek, Patrick J. Minx, Holland S. Cordum, Robert H. Waterston, Richard K. Wilson, and David C. Page. 2003. "Abundant Gene Conversion between Arms of Palindromes in Human and Ape Y Chromosomes." *Nature* 423 (6942): 873–76.
Sahlin, Kristoffer, and Veli Mäkinen. 2021. "Accurate Spliced Alignment of Long RNA Sequencing Reads." *Bioinformatics (Oxford, England)* 37 (24): 4643–51.
Sahlin, Kristoffer, Marta Tomaszkiewicz, Kateryna D. Makova, and Paul Medvedev. 2018. "Deciphering Highly Similar Multigene Family Transcripts from Iso-Seq Data with IsoCon." *Nature Communications* 9 (1): 4601.
Sakamoto, Takahiro, and Hideki Innan. 2022. "Muller's Ratchet of the Y Chromosome with Gene Conversion." *Genetics* 220 (1). https://doi.org/10.1093/genetics/iyab204.
Saxena, R., L. G. Brown, T. Hawkins, R. K. Alagappan, H. Skaletsky, M. P. Reeve, R. Reijo, S. Rozen, M. B. Dinulos, C. M. Disteche, and D. C. Page. 1996. "The DAZ Gene Cluster on the Human Y Chromosome Arose from an Autosomal Gene That Was Transposed, Repeatedly Amplified and Pruned." *Nature Genetics* 14 (3): 292–99.
Shi, Wentao, Sandra Louzada, Marina Grigorova, Andrea Massaia, Elena Arciero, Laura Kibena, Xiangyu Jack Ge, Yuan Chen, Qasim Ayub, Olev Poolamets, Chris Tyler-Smith, Margus Punab, Maris Laan, Fengtang Yang, Pille Hallast, and Yali Xue. 2019. "Evolutionary and Functional Analysis of RBMY1 Gene Copy Number Variation on the Human Y Chromosome." *Human Molecular Genetics* 28 (16): 2785–98.
Shi, Wentao, Andrea Massaia, Sandra Louzada, Juliet Handsaker, William Chow, Shane McCarthy, Joanna Collins, Pille Hallast, Kerstin Howe, Deanna M. Church, Fengtang Yang, Yali Xue, and Chris Tyler-Smith. 2019. "Birth, Expansion, and Death of VCY-Containing Palindromes on the Human Y Chromosome." *Genome Biology* 20 (1): 207.
Shumate, Alaina, Brandon Wong, Geo Pertea, and Mihaela Pertea. 2022. "Improved Transcriptome Assembly Using a Hybrid of Long and Short Reads with StringTie." *PLoS Computational Biology* 18 (6): e1009730.

Sim, Ngak-Leng, Prateek Kumar, Jing Hu, Steven Henikoff, Georg Schneider, and Pauline C. Ng. 2012. “SIFT Web Server: Predicting Effects of Amino Acid Substitutions on Proteins.” *Nucleic Acids Research* 40 (Web Server issue): W452–57.

Skaletsky, Helen, Tomoko Kuroda-Kawaguchi, Patrick J. Minx, Holland S. Cordum, Ladeana Hillier, Laura G. Brown, Sjoerd Repping, Tatyana Pyntikova, Johar Ali, Tamberlyn Bieri, Asif Chinwalla, Andrew Delehaunty, Kim Delehaunty, Hui Du, Ginger Fewell, Lucinda Fulton, Robert Fulton, Tina Graves, Shun-Fang Hou, Philip Latrielle, Shawn Leonard, Elaine Mardis, Rachel Maupin, John McPherson, Tracie Miner, William Nash, Christine Nguyen, Philip Ozersky, Kymberlie Pepin, Susan Rock, Tracy Rohlfing, Kelsi Scott, Brian Schultz, Cindy Strong, Aye Tin-Wollam, Shiaw-Pyng Yang, Robert H. Waterston, Richard K. Wilson, Steve Rozen, and David C. Page. 2003. “The Male-Specific Region of the Human Y Chromosome Is a Mosaic of Discrete Sequence Classes.” *Nature* 423 (6942): 825–37.

Smit, A. F. A., R. Hubley, and P. Green. 2021. “2013–2015. RepeatMasker Open-4.0.” https://scholar.google.com/citations?user=SOqGFioAAAAJ&hl=en&oi=sra.

Smith, G. P. 1976. “Evolution of Repeated DNA Sequences by Unequal Crossover.” *Science (New York, N.Y.)* 191 (4227): 528–35.

Smith, Martin D., Joel O. Wertheim, Steven Weaver, Ben Murrell, Konrad Scheffler, and Sergei L. Kosakovsky Pond. 2015. “Less Is More: An Adaptive Branch-Site Random Effects Model for Efficient Detection of Episodic Diversifying Selection.” *Molecular Biology and Evolution* 32 (5): 1342–53.

Soh, Y. Q. Shirleen, Jessica Alföldi, Tatyana Pyntikova, Laura G. Brown, Tina Graves, Patrick J. Minx, Robert S. Fulton, Colin Kremitzki, Natalia Koutseva, Jacob L. Mueller, Steve Rozen, Jennifer F. Hughes, Elaine Owens, James E. Womack, William J. Murphy, Qing Cao, Pieter de Jong, Wesley C. Warren, Richard K. Wilson, Helen Skaletsky, and David C. Page. 2014. “Sequencing the Mouse Y Chromosome Reveals Convergent Gene Acquisition and Amplification on Both Sex Chromosomes.” *Cell* 159 (4): 800–813.

Stouffs, Katrien, Willy Lissens, Greta Verheyen, Lisbet Van Landuyt, Annieta Goossens, Herman Tournaye, André Van Steirteghem, and Inge Liebaers. 2004. “Expression Pattern of the Y-Linked PRY Gene Suggests a Function in Apoptosis but Not in Spermatogenesis.” *Molecular Human Reproduction* 10 (1): 15–21.

Stouffs, K., W. Lissens, L. Van Landuyt, H. Tournaye, A. Van Steirteghem, and I. Liebaers. 2001. “Characterization of the Genomic Organization, Localization and Expression of Four PRY Genes (PRY1, PRY2, PRY3 and PRY4).” *Molecular Human Reproduction* 7 (7): 603–10.

Swanepoel, Callie M., and Jacob L. Mueller. 2024. “Out with the Old, in with the New: Meiotic Driving of Sex Chromosome Evolution.” *Seminars in Cell & Developmental Biology* 163 (November):14–21.

Swanepoel, Callie M., Gaojianyong Wang, Lucy Zhang, Björn Brändl, Hermann Bauer, Pavel Tsaytler, Franz-Josef Müller, Bernhard G. Herrmann, and Jacob L. Mueller. 2025. “Acquisition of Ampliconic Sequences Marks a Selfish Mouse T-Haplotype.” *bioRxivorg*. https://doi.org/10.1101/2025.01.28.635315.

Taguchi, Ayumu, Allen D. Taylor, Jaime Rodriguez, Müge Celiktaş, Hui Liu, Xiaotu Ma, Qing Zhang, Chee-Hong Wong, Alice Chin, Luc Girard, Carmen Behrens, Wan L. Lam, Stephen Lam, John D. Minna, Ignacio I. Wistuba, Adi F. Gazdar, and Samir M. Hanash. 2014. “A Search for Novel Cancer/testis Antigens in Lung Cancer Identifies VCX/Y Genes, Expanding the Repertoire of Potential Immunotherapeutic Targets.” *Cancer Research* 74 (17): 4694–4705.

Thibaud-Nissen, F., M. DiCuccio, W. Hlavina, A. Kimchi, P. A. Kitts, T. D. Murphy, K. D. Pruitt, and A. Souvorov. 2016. “P8008 The NCBI Eukaryotic Genome Annotation Pipeline.” *Journal of Animal Science* 94 (suppl_4): 184–184.

Tomaszkiewicz, Marta, Kristoffer Sahlin, Paul Medvedev, and Kateryna D. Makova. 2023. “Transcript Isoform Diversity of Ampliconic Genes on the Y Chromosome of Great Apes.” *Genome Biology and Evolution* 15 (11). https://doi.org/10.1093/gbe/evad205.

Trombetta, Beniamino, and Fulvio Cruciani. 2017. “Y Chromosome Palindromes and Gene Conversion.” *Human Genetics* 136 (5): 605–19.

Tse, J. Y. M., E. Y. M. Wong, A. N. Y. Cheung, W. S. O, P. C. Tam, and W. S. B. Yeung. 2003. “Specific Expression of VCY2 in Human Male Germ Cells and Its Involvement in the Pathogenesis of Male Infertility.” *Biology of Reproduction* 69 (3): 746–51.

Vallender, Eric J., and Bruce T. Lahn. 2004. “How Mammalian Sex Chromosomes Acquired Their Peculiar Gene Content.” *BioEssays: News and Reviews in Molecular, Cellular and Developmental Biology* 26 (2): 159–69.

Vaser, Robert, Ivan Sović, Niranjan Nagarajan, and Mile Šikić. 2017. “Fast and Accurate de Novo Genome

Assembly from Long Uncorrected Reads." *Genome Research* 27 (5): 737–46.
Vegesna, Rahulsimham, Marta Tomaszkiewicz, Paul Medvedev, and Kateryna D. Makova. 2019. "Dosage Regulation, and Variation in Gene Expression and Copy Number of Human Y Chromosome Ampliconic Genes." *PLoS Genetics* 15 (9): e1008369.
Vegesna, Rahulsimham, Marta Tomaszkiewicz, Oliver A. Ryder, Rebeca Campos-Sánchez, Paul Medvedev, Michael DeGiorgio, and Kateryna D. Makova. 2020. "Ampliconic Genes on the Great Ape Y Chromosomes: Rapid Evolution of Copy Number but Conservation of Expression Levels." *Genome Biology and Evolution* 12 (6): 842–59.
Veyrunes, Frédéric, Paul D. Waters, Pat Miethke, Willem Rens, Daniel McMillan, Amber E. Alsop, Frank Grützner, Janine E. Deakin, Camilla M. Whittington, Kyriena Schatzkamer, Colin L. Kremitzki, Tina Graves, Malcolm A. Ferguson-Smith, Wes Warren, and Jennifer A. Marshall Graves. 2008. "Bird-like Sex Chromosomes of Platypus Imply Recent Origin of Mammal Sex Chromosomes." *Genome Research* 18 (6): 965–73.
Wong, Elaine Y. M., Jenny Y. M. Tse, Kwok-Ming Yao, Po-Chor Tam, and William S. B. Yeung. 2002. "VCY2 Protein Interacts with the HECT Domain of Ubiquitin-Protein Ligase E3A." *Biochemical and Biophysical Research Communications* 296 (5): 1104–11.
Xue, Yali, and Chris Tyler-Smith. 2011. "An Exceptional Gene: Evolution of the TSPY Gene Family in Humans and Other Great Apes." *Genes* 2 (1): 36–47.
Ye, Danling, Arslan A. Zaidi, Marta Tomaszkiewicz, Kate Anthony, Corey Liebowitz, Michael DeGiorgio, Mark D. Shriver, and Kateryna D. Makova. 2018. "High Levels of Copy Number Variation of Ampliconic Genes across Major Human Y Haplogroups." *Genome Biology and Evolution* 10 (5): 1333–50.
Yoo, Dongahn, Arang Rhie, Prajna Hebbar, Francesca Antonacci, Glennis A. Logsdon, Steven J. Solar, Dmitry Antipov, Brandon D. Pickett, Yana Safonova, Francesco Montinaro, Yanting Luo, Joanna Malukiewicz, Jessica M. Storer, Jiadong Lin, Abigail N. Sequeira, Riley J. Mangan, Glenn Hickey, Graciela Monfort Anez, Parithi Balachandran, Anton Bankevich, Christine R. Beck, Arjun Biddanda, Matthew Borchers, Gerard G. Bouffard, Emry Brannan, Shelise Y. Brooks, Lucia Carbone, Laura Carrel, Agnes P. Chan, Juyun Crawford, Mark Diekhans, Eric Engelbrecht, Cedric Feschotte, Giulio Formenti, Gage H. Garcia, Luciana de Gennaro, David Gilbert, Richard E. Green, Andrea Guarracino, Ishaan Gupta, Diana Haddad, Junmin Han, Robert S. Harris, Gabrielle A. Hartley, William T. Harvey, Michael Hiller, Kendra Hoekzema, Marlys L. Houck, Hyeonsoo Jeong, Kaivan Kamali, Manolis Kellis, Bryce Kille, Chul Lee, Youngho Lee, William Lees, Alexandra P. Lewis, Qiuhui Li, Mark Loftus, Yong Hwee Eddie Loh, Hailey Loucks, Jian Ma, Yafei Mao, Juan F. I. Martinez, Patrick Masterson, Rajiv C. McCoy, Barbara McGrath, Sean McKinney, Britta S. Meyer, Karen H. Miga, Saswat K. Mohanty, Katherine M. Munson, Karol Pal, Matt Pennell, Pavel A. Pevzner, David Porubsky, Tamara Potapova, Francisca R. Ringeling, Joana L. Rocha, Oliver A. Ryder, Samuel Sacco, Swati Saha, Takayo Sasaki, Michael C. Schatz, Nicholas J. Schork, Cole Shanks, Linnéa Smeds, Dongmin R. Son, Cynthia Steiner, Alexander P. Sweeten, Michael G. Tassia, Françoise Thibaud-Nissen, Edmundo Torres-González, Mihir Trivedi, Wenjie Wei, Julie Wertz, Muyu Yang, Panpan Zhang, Shilong Zhang, Yang Zhang, Zhenmiao Zhang, Sarah A. Zhao, Yixin Zhu, Erich D. Jarvis, Jennifer L. Gerton, Iker Rivas-González, Benedict Paten, Zachary A. Szpiech, Christian D. Huber, Tobias L. Lenz, Miriam K. Konkel, Soojin V. Yi, Stefan Canzar, Corey T. Watson, Peter H. Sudmant, Erin Molloy, Erik Garrison, Craig B. Lowe, Mario Ventura, Rachel J. O'Neill, Sergey Koren, Kateryna D. Makova, Adam M. Phillippy, and Evan E. Eichler. 2025. "Complete Sequencing of Ape Genomes." *Nature* 641 (8062): 401–18.
Zhou, Ran, David Macaya-Sanz, Craig H. Carlson, Jeremy Schmutz, Jerry W. Jenkins, David Kudrna, Aditi Sharma, Laura Sandor, Shengqiang Shu, Kerrie Barry, Gerald A. Tuskan, Tao Ma, Jianquan Liu, Matthew Olson, Lawrence B. Smart, and Stephen P. DiFazio. 2020. "A Willow Sex Chromosome Reveals Convergent Evolution of Complex Palindromic Repeats." *Genome Biology* 21 (1): 38.
Zhu, Zexian, Lubna Younas, and Qi Zhou. 2025. "Evolution and Regulation of Animal Sex Chromosomes." *Nature Reviews. Genetics* 26 (1): 59–74.
Zou, Sheng Wei, Jian Chao Zhang, Xiao Dong Zhang, Shi Ying Miao, Shu Dong Zong, Qi Sheng, and Lin Fang Wang. 2003. "Expression and Localization of VCX/Y Proteins and Their Possible Involvement in Regulation of Ribosome Assembly during Spermatogenesis." *Cell Research* 13 (3): 171–77.

Table 1. Homologs of Y ampliconic gene families. Y: Y chromosome, X: X chromosome, A: Autosomes. The number of copies for non-Y homologs is shown as subscripts if more than one was found. The number of YAG copies is given in Table S4. Bold in column Origin indicates that our observations support the previously reported origin of the gene family.

Gene family	Bonobo	Chimpanzee	Human	Gorilla	Bornean orangutan	Sumatran orangutan	Siamang	Origin
BPY2	Y	Y	Y	Y	–	–	–	NF (35 MYA)[A]
CDY	Y, A_2	Y, A_2	Y, A_2	Y, A_2	Y, A_2	Y, A_2	Y, A_2	**RP of *CDYL* (159±13 MYA)[B]**
DAZ	Y, A_2	Y, A_2	Y, A_2	Y, A_2	Y, A_2	Y, A_2	Y, A_2	**TP of *DAZL*[B] (38 MYA[C])**
HSFY	–	–	Y	Y	Y	Y	Y	RP of *HSFYL*[B]
RBMY*	X_4,Y, A_7	X_3,Y, A_7	X_3,Y, A_7	X_3,Y, A_7	X_4,Y, A_7	X_4,Y, A_8	X_3,Y, A_8	**XY[D]**
TSPY	Y	Y	Y	Y	Y	Y	Y	TP of *TSPYL*, XY[B]
VCY	X_{16}, Y	X_{11}, Y	X_4, Y	X_4	X_8	X_7	X_6, Y, A	**XY[E]**

*For *RBMY*, the RNA-binding domain clustered with many autosomal genes. However, only the X paralogs shared homology extending outside the RNA-binding domain.
RP = Retrotransposition, TP = Transposition, NF = Neofunctionalization. XY = Originating from the proto-sex chromosome pair. MYA = Million years ago.
A(Cao et al. 2015), B(Bhowmick et al. 2007),C(Hughes et al. 2012) , D(Elliott et al. 2019), E(Iwase et al. 2010)

Table 2. Selection analysis of YAG families. Sequences: Number of all sequences/number of unique sequences considered for the analysis. Codons: number of codons analyzed. *dN*/*dS* CI: 95% confidence intervals for the *dN*/*dS* analysis. Mean *dN*/*dS* ≠ 1: *p*-value for the alternative hypothesis that the alignment-wide and tree-wide *dN*/*dS* is different from 1. Branch heterogeneity: to test for variation in selection pressure across lineages, a local MG94 model (with separate *dN/dS* for each branch) was fitted and compared to the global MG94 model (single *dN/dS* across the tree) using a Likelihood Ratio Test, whose *p*-value is shown. BUSTED-E: the *p*-value for a gene-wide test for episodic diversifying selection. aBSREL: the number of individual branches with evidence of episodic diversifying selection. MEME-selected sites: the number of individual sites that have evidence of episodic diversifying selection.

Gene family	Sequences	Codons	Mean *dN/dS* (CI)	*p*-values			aBSREL-selected branches ($p \leq 0.05$)	MEME-selected sites ($p \leq 0.05$)
				Mean *dN*/*dS* ≠ 1	Branch hetero-geneity	BUSTED-E*		
BPY2	8/4	107	0.63 (0.20-1.47)	0.562	0.56	0.5	0	0
CDY	63/45	540	0.40 (0.36-0.44)	**$<1\times10^{-10}$**	**5.23×10^{-07}**	0.165	0	6
DAZ RRM	73/36	165	0.60 (0.50-0.71)	**0.001**	0.03	0.5	0	1
DAZ repeats	256/54	30	0.97 (0.76-1.21)	0.885	0.81	0.5	0	1
HSFY	21/13	403	0.43 (0.33-0.55)	**2.11×10^{-04}**	0.48	0.5	0	0
RBMY	83/55	400	0.50 (0.45-0.54)	**$<1\times10^{-10}$**	**6.43×10^{-07}**	**0.03****	1	15
TSPY	163/60	276	0.77 (0.64-0.91)	0.117	0.86	0.5	0	2
VCY	63/41	147	1.04 (0.87-1.24)	0.833	0.88	0.465	0	2

*No anomalies were detected by the BUSTED-E test except for a single site in the *VCY* gene (Figure S19).
**The significant result of BUSTED-E in *RBMY* is mainly driven by multi-nucleotide variation at codon 248. Without this codon, the test is no longer significant.

Figure 1. Inter- and intraspecies variation in copy number of Y ampliconic genes. Copy number is plotted on the X axis, and the proportion of individuals on the Y axis. A vertical line was used when only one individual per species was available.

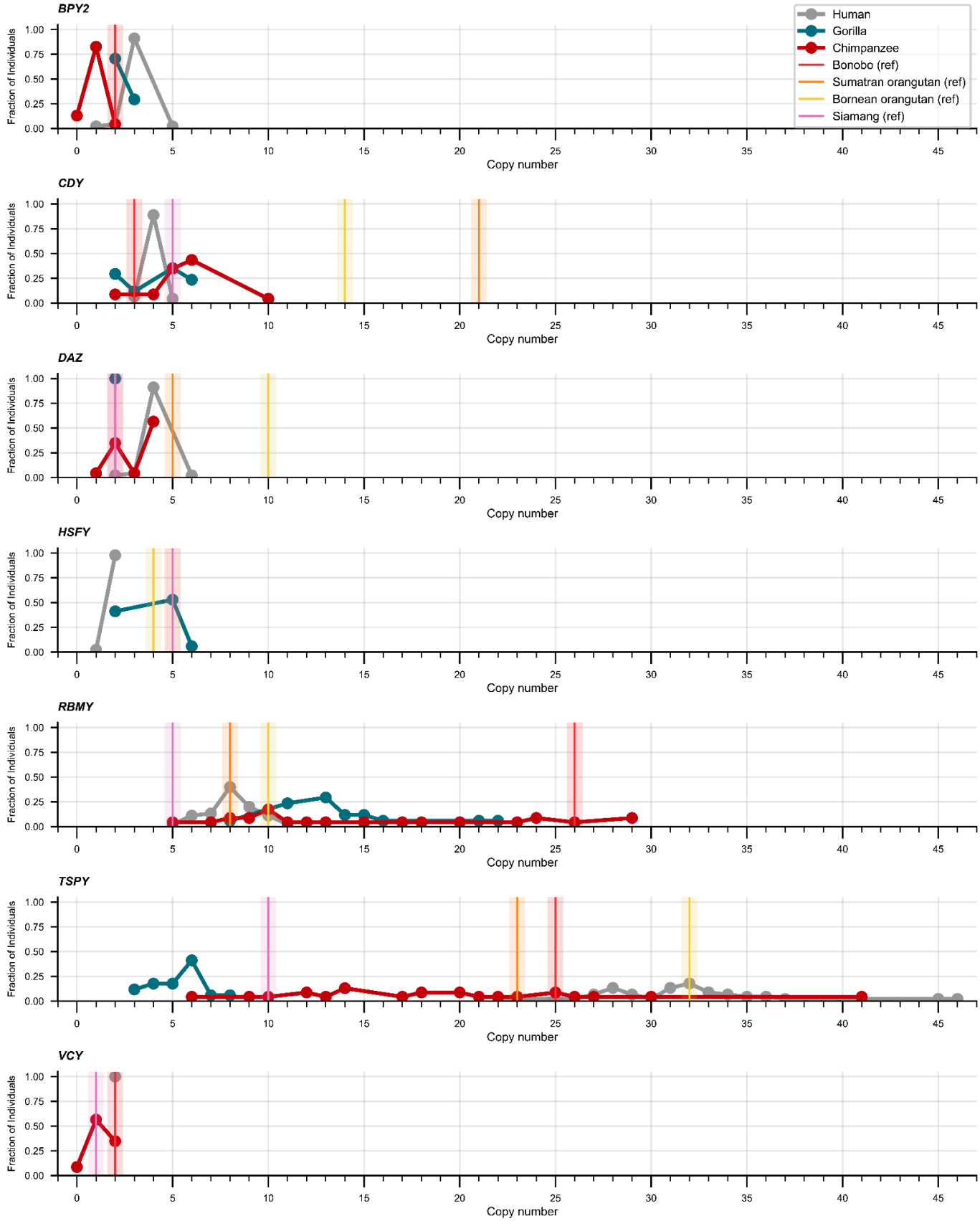

Figure 2. Chromosomal organization of YAGs. (**A**) Two models of homogenization of ampliconic genes via intrachromosomal recombination between palindrome arms and between direct repeats in tandemly repeated arrays. (**B**) Violin plots showing the distribution of pairwise sequence identities and pairwise permutation test results comparing sequence identity for protein-coding sequences of gene copies from the same gene family and from the same species. The analysis was performed across gene copies located within tandem arrays (1,391 comparisons across 136 gene copies), from different arrays (297 comparisons across 69 gene copies), located on opposite arms of the same palindromes (44 comparisons across 80 gene copies; gene copies were compared only if they were in the opposite orientation), on the same arm of a palindrome (10 comparisons across 20 gene copies), within different palindromes (446 comparisons across 78 gene copies), and outside of palindromes and arrays (89 comparisons across 55 genes). For underlying data, see Table S19. (**C**) Phylogenetic trees of seven YAG gene families: *DAZ* RRMs, *CDY*, and *RBMY* (left column, shared interrupted scale); *TSPY* (center column); and *BPY2*, *HSFY*, and *VCY* (right column, shared scale). Trees of *DAZ* RRM and *CDY* were rooted with the closest autosomal paralogue (*DAZL* and *CDYL,* respectively). The *RBMY* tree was rooted with the X-linked paralogue (*RBMX*). All other trees were rooted with Y-chromosome homologs from the most distantly related species (gorilla in *BPY*, siamang in *HSFY*, *TSPY*, and *VCY*). The color of external nodes indicates species. Circles denote non-palindromic gene copies; triangles denote copies residing within a palindrome. A ring surrounding a node indicates that the gene copy is located within a tandemly repeated array. Curved arches connect the two arms (A and B) of the same palindrome within a species. In the left column, the scale is compressed below 0.22 and above 0.29 substitutions per site to accommodate the wide range of branch lengths while preserving resolution in the intermediate range; gray vertical lines mark 0.1 substitutions/site intervals. Trees in the left column are horizontally aligned at the positions of their respective outgroup nodes (blue vertical lines) to facilitate comparison of within-family diversification.

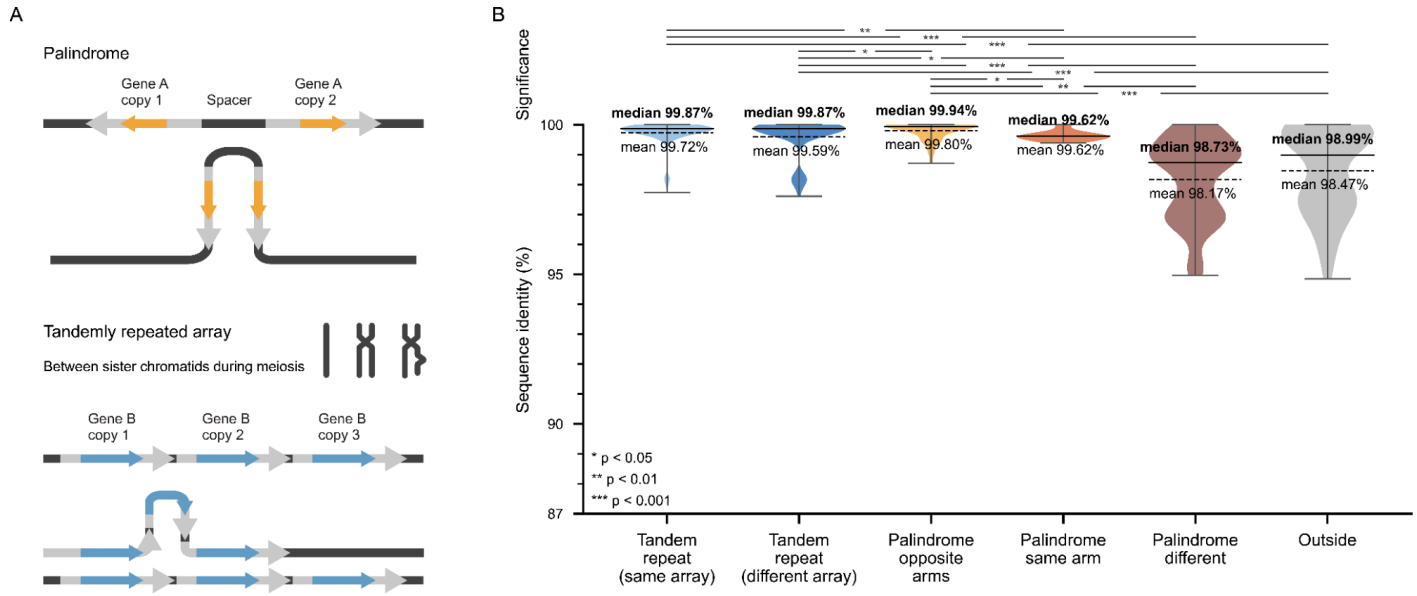

C

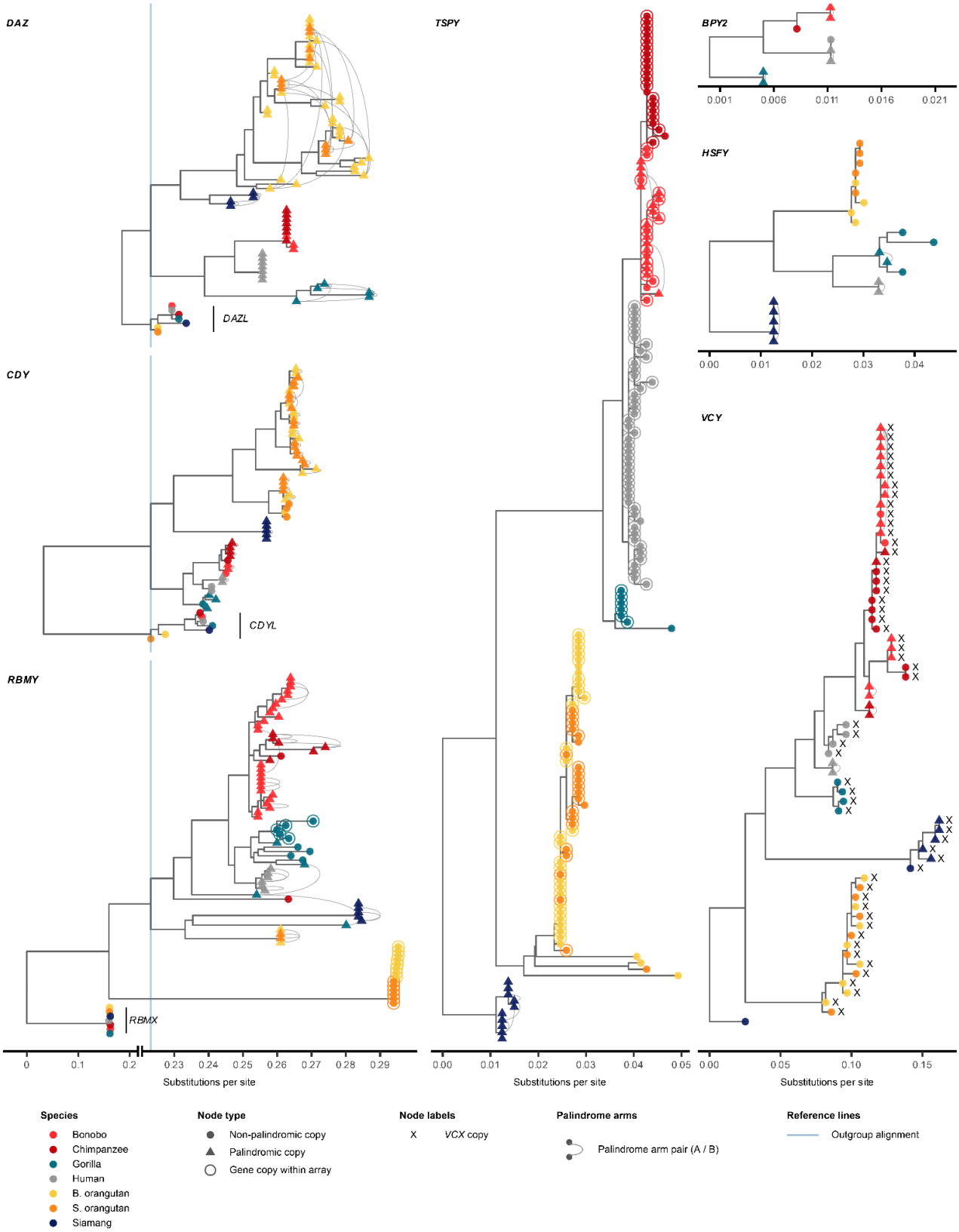
DAZ
DAZL
CDY
CDYL
RBMY
RBMX
TSPY
BPY2
HSFY
VCY
0 0.1 0.2 0.23 0.24 0.25 0.26 0.27 0.28 0.29
Substitutions per site
0.00 0.01 0.02 0.03 0.04 0.05
Substitutions per site
0.001 0.006 0.011 0.016 0.021
0.00 0.01 0.02 0.03 0.04
0.00 0.05 0.10 0.15
Substitutions per site
Species
Bonobo
Chimpanzee
Gorilla
Human
B. orangutan
S. orangutan
Siamang
Node type
Non-palindromic copy
Palindromic copy
Gene copy within array
Node labels
X VCX copy
Palindrome arms
Palindrome arm pair (A / B)
Reference lines
Outgroup alignment

Figure 3. Distribution of structural and sequence RNA isoforms of YAGs. (**A**) Structural transcript isoforms for six gene families (*BPY2*, *CDY*, *HSFY*, *RBMY*, *TSPY*, and *VCY*). Each isoform was aligned to a single human reference copy. Colored rectangles denote RNA sequence aligned to exons, and introns are shown as gray lines. Intronic sequences without aligned RNA sequences are collapsed. Each color represents a distinct structural isoform for each YAG family. Human reference gene copies are shown under the colored isoforms: thicker black boxes represent the coding sequence, whereas thinner gray blocks represent UTRs. The burgundy color represents *RBMY*'s SRGY-box containing 111-bp exon repeat units (Ma et al. 1993; Elliott 2004). (**B**) Each panel displays the relative sequence isoform usage (individual bars) for a given gene family (rows) and species (columns). Colors distinguish individual structural isoforms within each gene family, as indicated by legends on the right (color scheme matching part A). Stacked bars represent the proportion of reads supporting each structural isoform for a given sequence isoform, normalized to the total number of classified reads at that panel (left y-axis, 0–100%). The light gray shading on each panel indicates the total read depth for a YAG family in a sample from a given species (right y-axis, total counts). (**C**) *DAZ* transcript isoforms. Each horizontal bar represents a unique *DAZ* transcript isoform, aligned at the rightmost RRM domain. Dark gray blocks indicate RRM domains; colored blocks indicate *DAZ* repeat units, with each color representing a distinct repeat sequence variant shared across two or more species. Gray repeat blocks are species-specific variants. Repeat units embedded between RRM domains are also shown and labeled. Uppercase letters identify repeat variants occurring after the RRM motifs; lowercase letters denote inter-RRM repeat variants. Sumatran orangutan *DAZ* expression levels were too low to draw a conclusion. "*" indicates Pongo-specific *RBMY* isoforms.

A

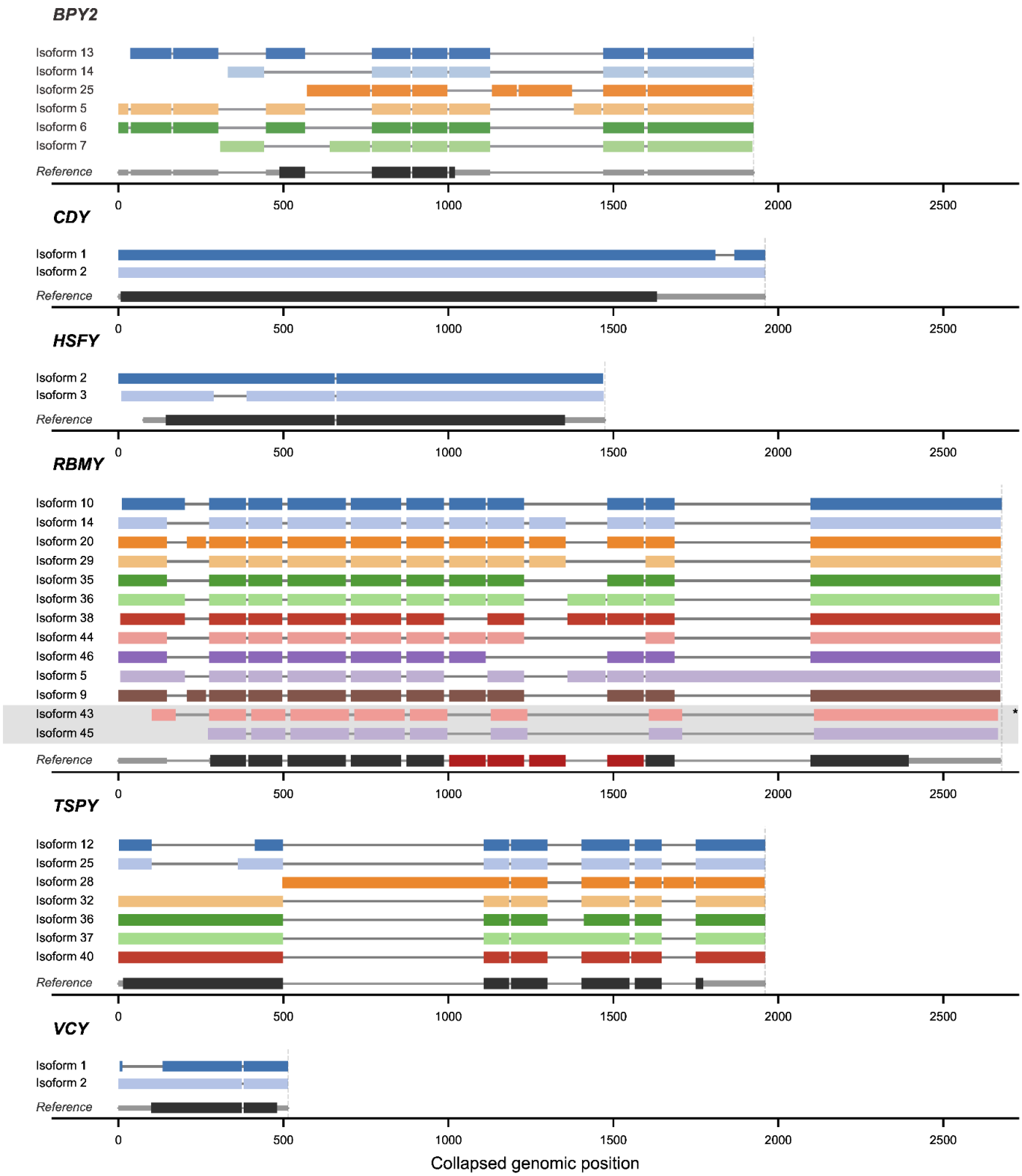
BPY2
Isoform 13
Isoform 14
Isoform 25
Isoform 5
Isoform 6
Isoform 7
Reference
0
500
1000
1500
2000
2500
CDY
Isoform 1
Isoform 2
Reference
HSFY
Isoform 2
Isoform 3
Reference
RBMY
Isoform 10
Isoform 14
Isoform 20
Isoform 29
Isoform 35
Isoform 36
Isoform 38
Isoform 44
Isoform 46
Isoform 5
Isoform 9
Isoform 43
Isoform 45
*
Reference
TSPY
Isoform 12
Isoform 25
Isoform 28
Isoform 32
Isoform 36
Isoform 37
Isoform 40
Reference
VCY
Isoform 1
Isoform 2
Reference
Collapsed genomic position

B

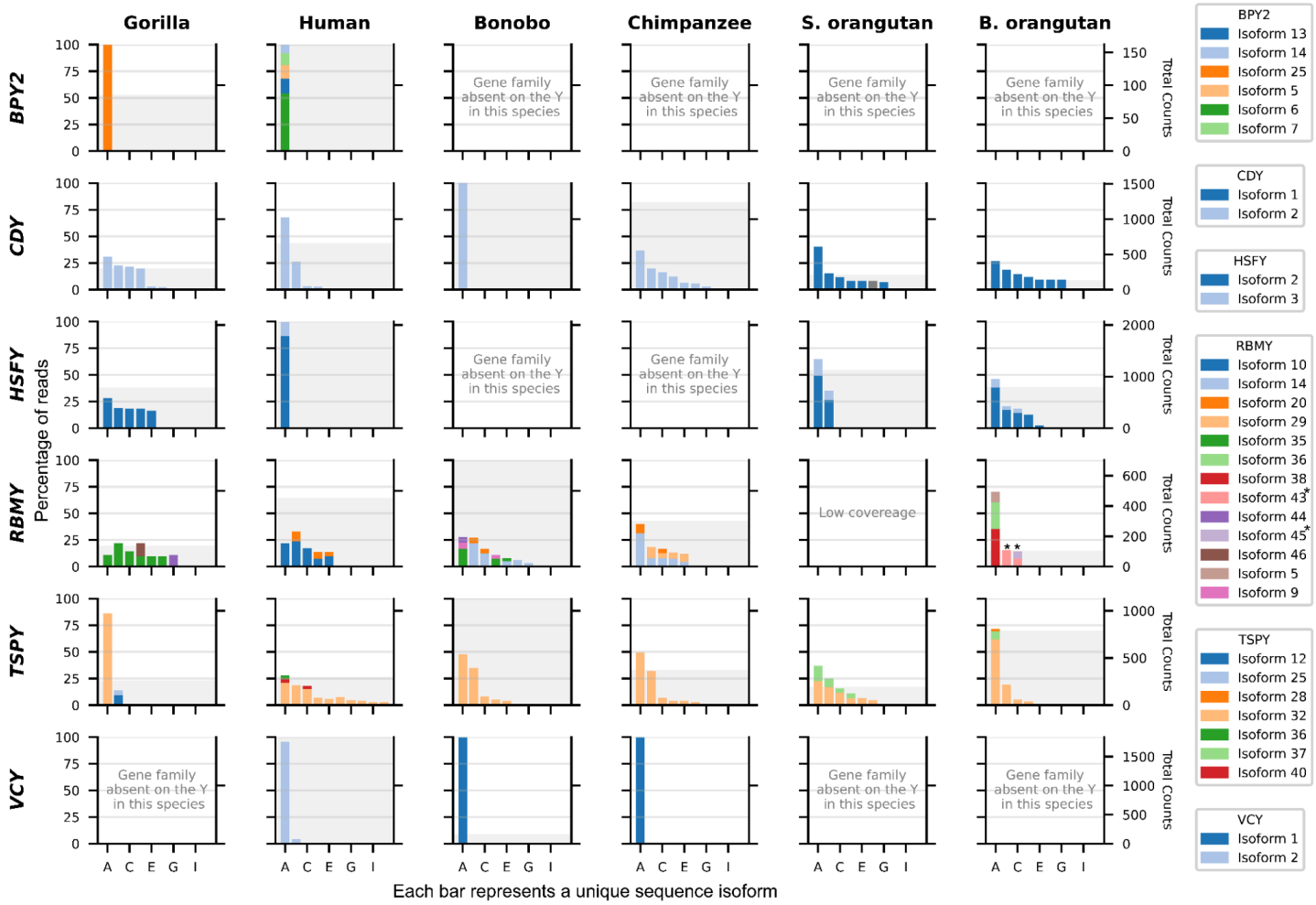
Gorilla
Human
Bonobo
Chimpanzee
S. orangutan
B. orangutan
BPY2
CDY
HSFY
RBMY
TSPY
VCY
Percentage of reads
Total Counts
Gene family absent on the Y in this species
Low covereage
A C E G I
Each bar represents a unique sequence isoform
BPY2
Isoform 13
Isoform 14
Isoform 25
Isoform 5
Isoform 6
Isoform 7
CDY
Isoform 1
Isoform 2
HSFY
Isoform 2
Isoform 3
RBMY
Isoform 10
Isoform 14
Isoform 20
Isoform 29
Isoform 35
Isoform 36
Isoform 38
Isoform 43*
Isoform 44
Isoform 45*
Isoform 46
Isoform 5
Isoform 9
TSPY
Isoform 12
Isoform 25
Isoform 28
Isoform 32
Isoform 36
Isoform 37
Isoform 40
VCY
Isoform 1
Isoform 2

C

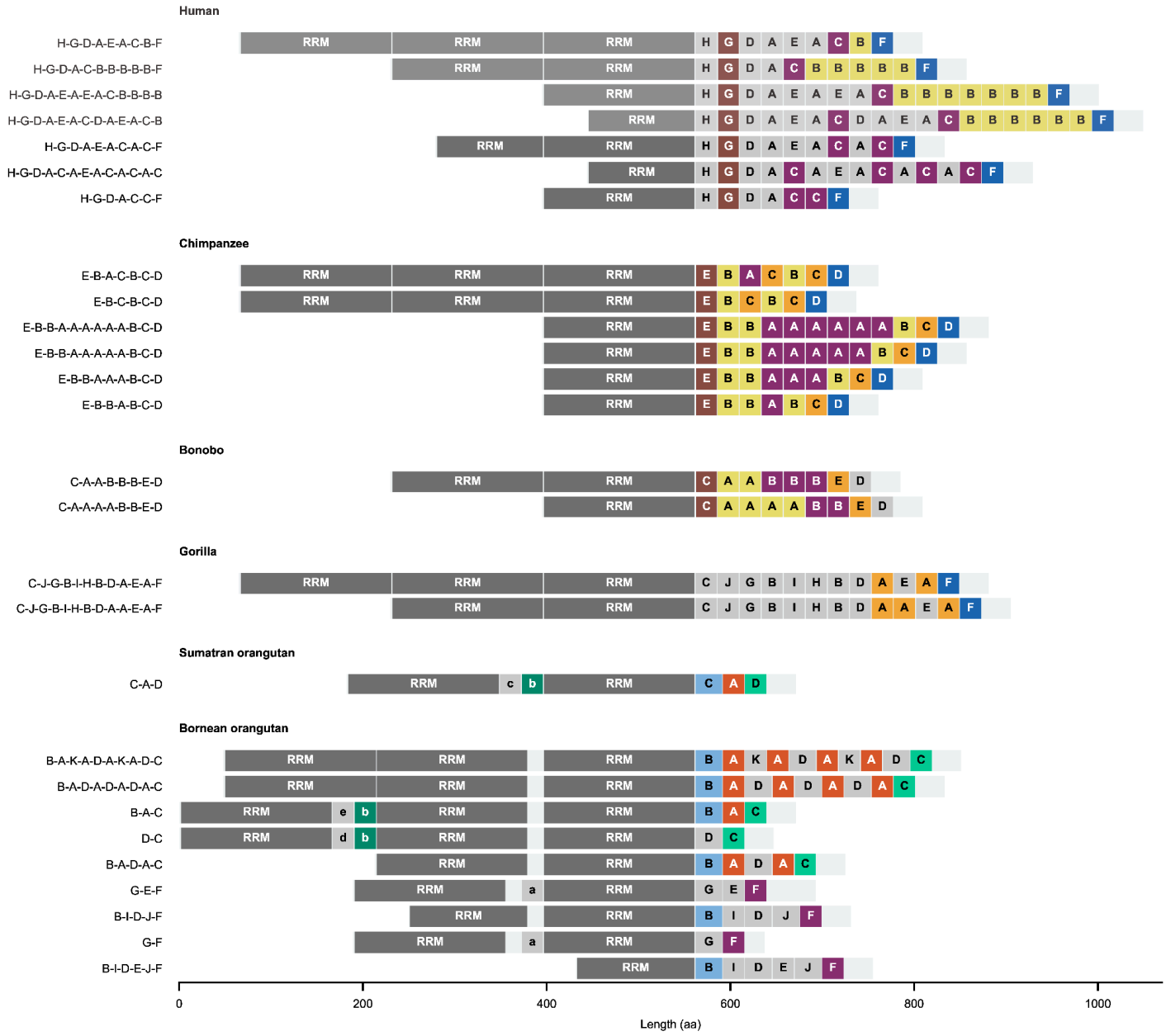
Human
H-G-D-A-E-A-C-B-F
H-G-D-A-C-B-B-B-B-F
H-G-D-A-E-A-E-A-C-B-B-B
H-G-D-A-E-A-C-D-A-E-A-C-B
H-G-D-A-E-A-C-A-C-F
H-G-D-A-C-A-E-A-C-A-C-A-C
H-G-D-A-C-C-F
Chimpanzee
E-B-A-C-B-C-D
E-B-C-B-C-D
E-B-B-A-A-A-A-A-A-B-C-D
E-B-B-A-A-A-A-A-A-B-C-D
E-B-B-A-A-A-B-C-D
E-B-B-A-B-C-D
Bonobo
C-A-A-B-B-B-E-D
C-A-A-A-A-B-B-E-D
Gorilla
C-J-G-B-I-H-B-D-A-E-A-F
C-J-G-B-I-H-B-D-A-A-E-A-F
Sumatran orangutan
C-A-D
Bornean orangutan
B-A-K-A-D-A-K-A-D-C
B-A-D-A-D-A-D-A-C
B-A-C
D-C
B-A-D-A-C
G-E-F
B-I-D-J-F
G-F
B-I-D-E-J-F
RRM
0
200
400
600
800
1000
Length (aa)

Figure 4. Protein isoforms and confidence levels of structures predicted with ColabFold. (**A**) pLDDT (per-residue measure of local confidence) scores from AlphaFold2 (Jumper et al. 2021) were projected onto the genomic exon-intron diagrams (from Figure 3A and Figure S10 for *DAZ*). The resulting per-nucleotide pLDDT traces are rendered as colored line segments above each isoform, using a red–white–blue color scale shown in the figure. (**B**) Relationships between transcript isoforms, protein isoforms, and structure-derived protein clusters. Each subplot—one for each gene family—comprises three columns connected with ribbons. Column one consists of bars representing unique transcript isoforms. For *BPY2, CDY*, *HSFY*, *RBMY*, *TSPY*, and *VCY*, the color of the bars is derived from the structural isoform the transcript represents based on panel A. Multiple bars of the same color represent multiple sequence isoforms of the same structure. Bars in the second column represent protein isoforms, and color ribbons between columns one and two connect transcript isoforms with their respective protein translations. Transcripts resulting in identical proteins (shared reading frame, differing only by synonymous mutations) are collapsed and colored by the most abundant transcript (according to read count). Finally, the third column represents clusters of proteins derived from their 3D structures using Foldseek (van Kempen et al. 2024). Ribbons connect protein isoforms from column two, contributing to clusters in column three. Colors of bars in the third column are derived by mixing the colors of ribbons leading into them. Colors of transcript and protein isoforms for the *DAZ* gene are derived from the cluster they contribute to. Three main clusters C1, C2, and C3 represent *DAZ* proteins with two, one, and three RRMs, respectively. (**C**) Molecular visualization of the dominant cluster of five highly ordered YAG proteins created with PyMol (The PyMOL Molecular Graphics System, Version 1.2r3pre, Schrödinger, LLC.). Seven sites highlighted in yellow show evidence of episodic diversifying selection according to the MEME model (Murrell et al. 2012) and are predicted by SIFT (Sim et al. 2012) to affect protein function with high confidence (Table S12).

A

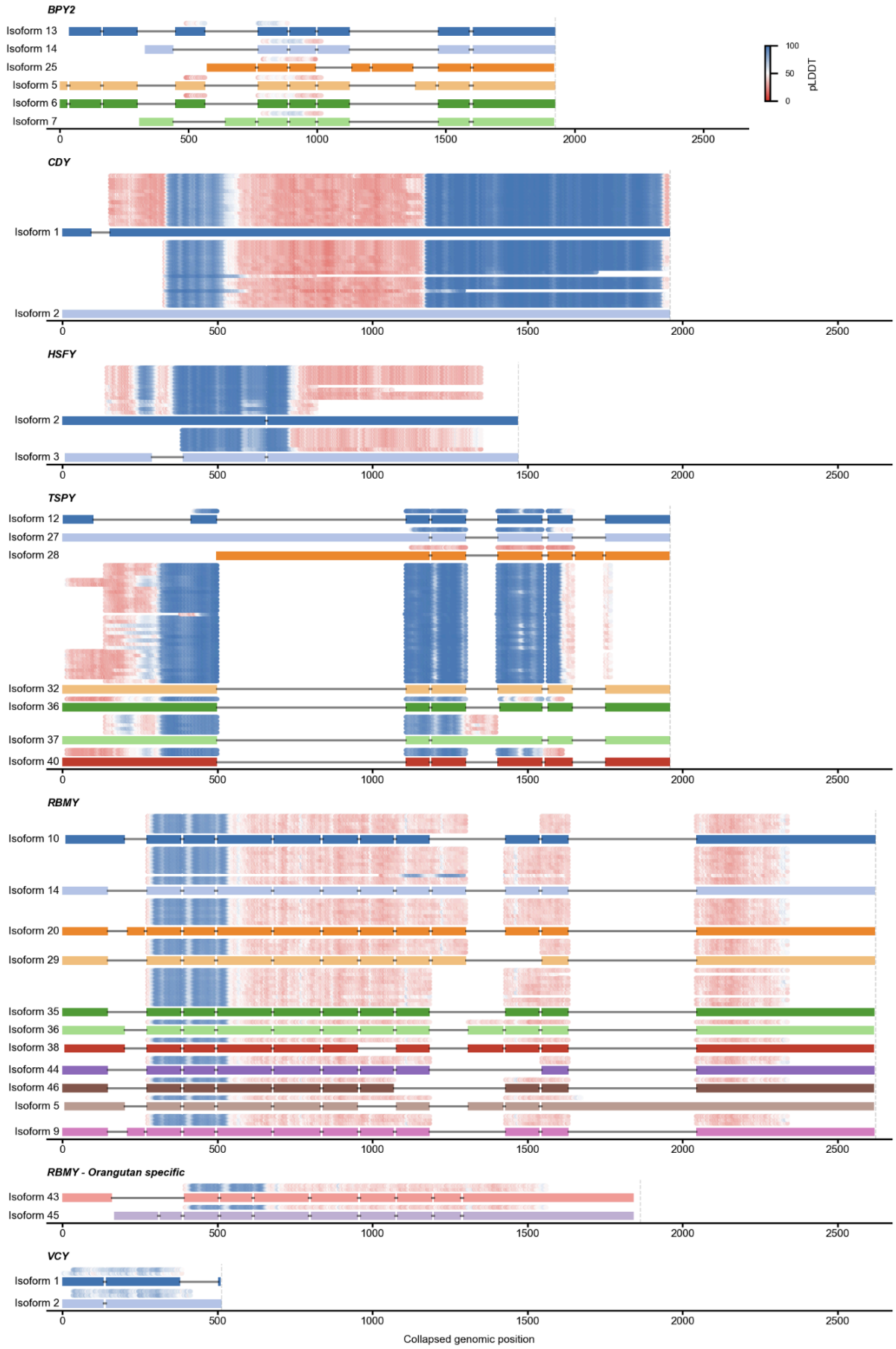
BPY2
Isoform 13
Isoform 14
Isoform 25
Isoform 5
Isoform 6
Isoform 7
100
50
0
pLDDT
CDY
Isoform 1
Isoform 2
HSFY
Isoform 2
Isoform 3
TSPY
Isoform 12
Isoform 27
Isoform 28
Isoform 32
Isoform 36
Isoform 37
Isoform 40
RBMY
Isoform 10
Isoform 14
Isoform 20
Isoform 29
Isoform 35
Isoform 36
Isoform 38
Isoform 44
Isoform 46
Isoform 5
Isoform 9
RBMY - Orangutan specific
Isoform 43
Isoform 45
VCY
Isoform 1
Isoform 2
0
500
1000
1500
2000
2500
Collapsed genomic position

B

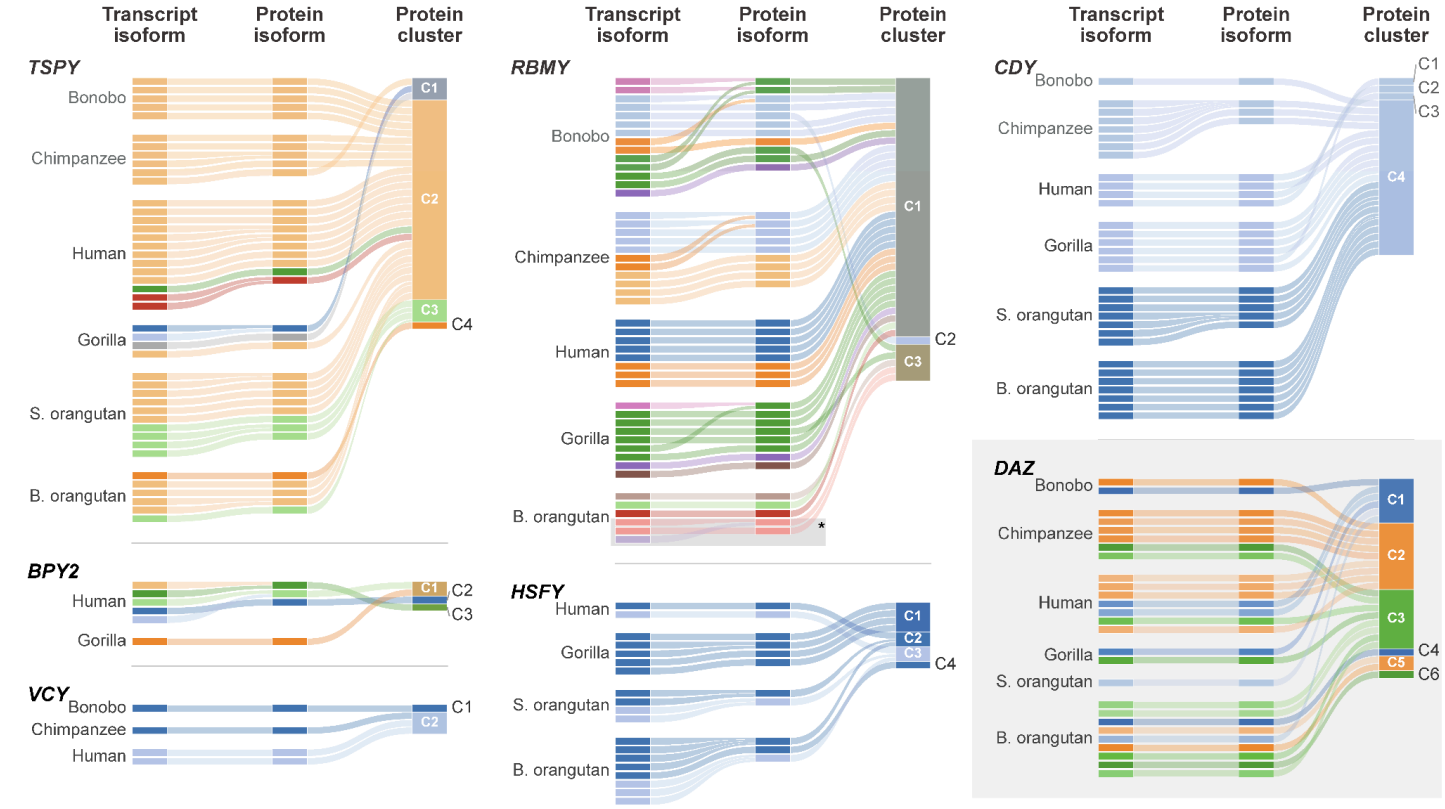
Transcript isoform
Protein isoform
Protein cluster
TSPY
Bonobo
Chimpanzee
Human
Gorilla
S. orangutan
B. orangutan
C1
C2
C3
C4
BPY2
Human
Gorilla
C1
C2
C3
VCY
Bonobo
Chimpanzee
Human
C1
C2
RBMY
Bonobo
Chimpanzee
Human
Gorilla
B. orangutan
C1
C2
C3
*
HSFY
Human
Gorilla
S. orangutan
B. orangutan
C1
C2
C3
C4
CDY
Bonobo
Chimpanzee
Human
Gorilla
S. orangutan
B. orangutan
C1
C2
C3
C4
DAZ
Bonobo
Chimpanzee
Human
Gorilla
S. orangutan
B. orangutan
C1
C2
C3
C4
C5
C6

C

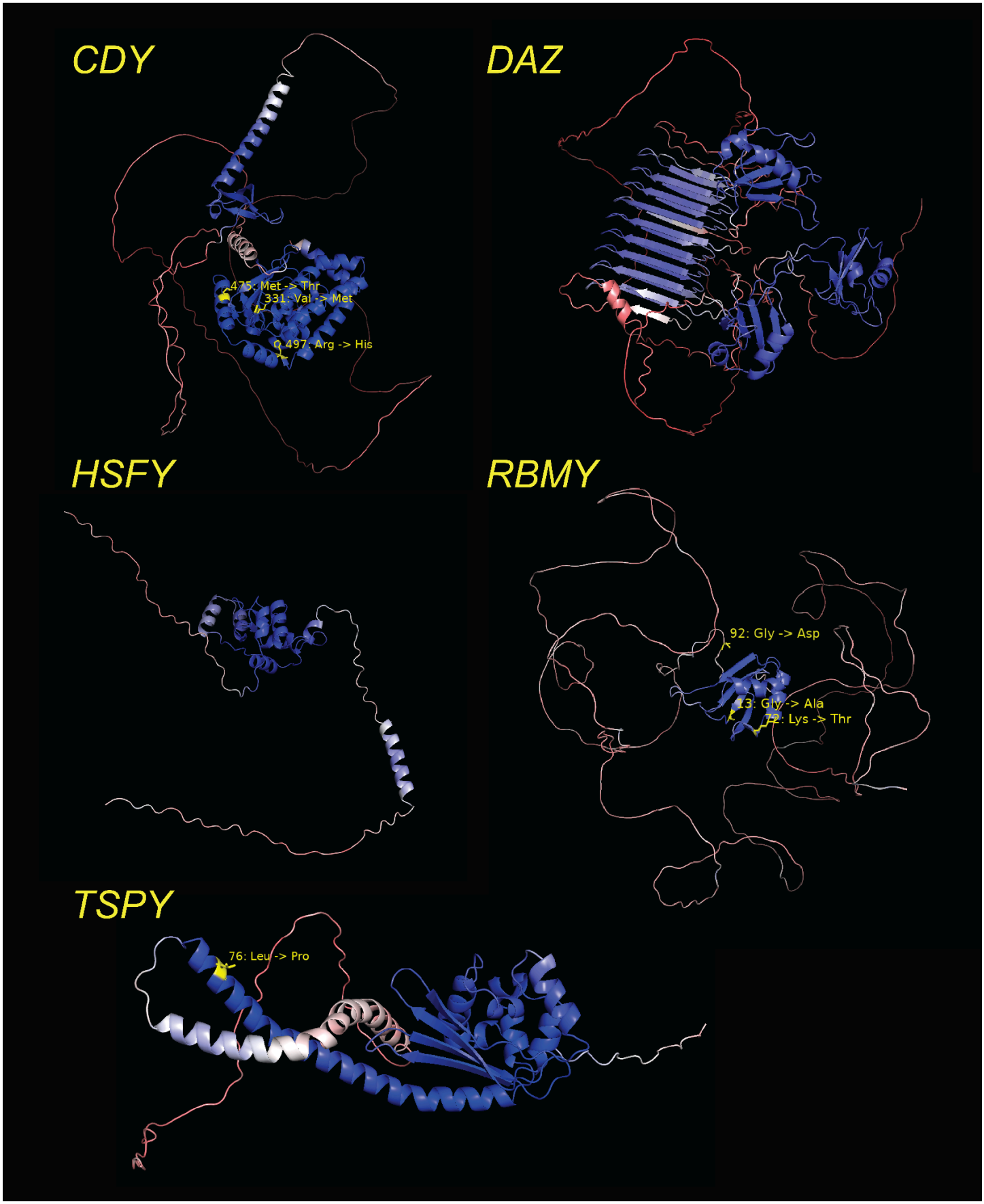
CDY
475: Met -> Thr
331: Val -> Met
497: Arg -> His
DAZ
HSFY
RBMY
92: Gly -> Asp
13: Gly -> Ala
72: Lys -> Thr
TSPY
76: Leu -> Pro